

Optical off-nuclear spectra of quasar hosts and radio galaxies

David H. Hughes^{1*}, Marek J. Kukula¹, James S. Dunlop¹ and Todd Boroson²

¹ *Institute for Astronomy, Department of Physics and Astronomy, University of Edinburgh, Blackford Hill, Edinburgh EH9 3HJ, U.K.*

² *NOAO, PO Box 26732, Tucson, Arizona 85726-6732, U.S.A.*

ABSTRACT

We present optical ($\sim 3200\text{\AA}$ to $\sim 9000\text{\AA}$) off-nuclear spectra of 26 powerful active galaxies in the redshift range $0.1 \leq z \leq 0.3$, obtained with the Mayall and William Herschel 4-meter class telescopes. The sample consists of radio-quiet quasars, radio-loud quasars (all with $-23 \geq M_V \geq -26$) and radio galaxies of Fanaroff & Riley Type II (with extended radio luminosities and spectral indices comparable to those of the radio-loud quasars). The spectra were all taken approximately 5 arcseconds off-nucleus, with offsets carefully selected so as to maximise the amount of galaxy light falling into the slit, whilst simultaneously minimising the amount of scattered nuclear light. The majority of the resulting spectra appear to be dominated by the integrated stellar continuum of the underlying galaxies rather than by light from the non-stellar processes occurring in the active nuclei, and in many cases a 4000\AA break feature can be identified. The individual spectra are described in detail, and the importance of the various spectral components is discussed. Stellar population synthesis modelling of the spectra will follow in a subsequent paper (Nolan et al. 2000).

Key words: galaxies: stellar content – galaxies: active – quasars: general

1 INTRODUCTION

Understanding the host galaxies of active galactic nuclei (AGN) is now recognised as an important step on the path towards reaching an understanding of AGN themselves - how they form, how they are fuelled and how the differences between the various classes of object arise. In two areas in particular the nature of the host galaxy gives us a direct insight into the workings of the AGN: galaxy properties seem to play a role in determining the radio loudness of the central engine (powerful radio sources are almost never found in spiral or disc-dominated systems – though see McHardy et al. 1994); and amongst radio-loud objects the host galaxies offer a powerful, orientation-independent means of testing models which attempt to unify different types of AGN via beaming and viewing angle effects (*eg* Urry & Padovani 1995). The observations presented here attempt to address both of these issues by comparing the galaxies associated with the three main types of powerful AGN: radio-quiet quasars (RQQs), radio-loud quasars (RLQs) and radio galaxies (RGs) of Fanaroff & Riley Type II.

1.1 Quasar hosts

Only once the problem of separating the diffuse galaxy emission from the wings of the quasar point spread function (PSF) has been overcome can one begin to describe and classify the morphologies, brightness profiles and interaction histories of the quasar hosts. Over the last decade improvements in ground-based techniques and the advent of the Hubble Space Telescope (HST) have revolutionised our understanding of quasar host galaxies.

Evidence for mergers or interactions in the form of morphological disturbances and close companions is a common feature of these images, but a significant number of quasars are also found in what appear to be undisturbed hosts. In addition, the idea that radio-loudness is a straightforward consequence of the host galaxy type has had to be abandoned. Although some radio-quiet quasars are found in spirals (*eg* Hutchings et al. 1994; Örndahl, Rönnback & van Groningen 1997) in general the hosts of both radio-loud and radio-quiet quasars tend to have properties consistent with early-type galaxies (*eg* Véron-Cetty & Woltjer 1990; Disney et al. 1995, Hutchings & Morris 1995, Bahcall et al. 1997, McLeod, Rieke & Storrie-Lombardi 1999) and typically have luminosities $> L^*$ (*eg* Dunlop et al. 1993, Bahcall, Kirhakos & Schneider 1994, 1995ab, 1996; Hutchings et al.

* current address: INAOE, Apartado Postal 51 y 216, 7200, Puebla, Pue., Mexico

1994, Boyce et al. 1998, Hooper, Impey & Foltz 1997) and in many cases are comparable in mass to brightest cluster galaxies (BCGs).

Meanwhile, McLeod & Rieke (1995a) find evidence for a *lower* limit on the *H*-band luminosities (and hence the mass of the red, established stellar populations) of galaxies hosting radio-quiet AGN, which appears to increase as the nuclear luminosity increases, implying that the nuclear activity is closely linked to the mass of the bulge component of the host. This impression has been reinforced by McLure et al. (1999), who find that *all* the RQQs with $M_R \leq -24$ in their HST sample occur in massive elliptical galaxies, with only the least luminous radio-quiet objects lying in disc-dominated hosts.

Many long-held views about the triggering of nuclear activity and the origins of radio loudness are currently being reassessed in the light of these imaging studies, but images cannot tell the whole story. A completely independent way of characterising the host galaxies of AGN is via analysis and classification of their stellar populations and starformation histories. The aim of the observations described in this paper was to obtain high signal-to-noise spectra of quasar hosts and radio galaxies for use in spectrophotometric modelling to determine the nature and history of their stellar constituents.

1.2 Spectroscopy of quasar hosts

Previous off-nuclear spectroscopy of the host galaxies of quasars has produced mixed results. Boroson & Oke (1982) were the first to detect an unequivocally stellar continuum from the nebulosity surrounding the radio-loud quasar 3C48 and subsequent studies revealed stellar continua and emission/absorption features around several other quasars (Boroson, Oke & Green 1982; Boroson & Oke 1984; Boroson, Persson & Oke 1985; Hickson & Hutchings 1987; Hutchings & Crampton 1990). However, except for the general result that there appeared to be systematic differences between the spectra of radio-loud and radio-quiet quasar hosts, these studies produced little advance in our understanding of the relationship between RQQs, RLQs and RGs for the reasons outlined below.

In general the quasar targets were chosen virtually at random, often for the sole reason that they were ‘interesting’ and/or unusual. Until now a programme of off-nuclear spectroscopy for statistically useful and properly matched samples of RQQs and RLQs has never been carried out, nor has any attempt been made to compare the off-nuclear spectra of RLQs with equivalent *off-nuclear* spectra of radio galaxies.

The early work also focussed mostly on emission-line activity, with discussion of the stellar continuum being confined to classification as red or blue, and the identification of a few stellar features. Only limited attempts were made to use the form of the spectrum to investigate the composition and evolution of the stellar population.

Finally, few of the host galaxy spectra were taken sufficiently off-nucleus - *eg* the spectra taken by Boroson and collaborators were taken only $3''$ from the quasar. This was done in the belief that any further off-nucleus the host galaxy would be too faint for a reasonable spectrum to be obtained, but inevitably resulted in significant contamination of the

host galaxy spectrum by scattered light from the quasar nucleus. A scaled version of the quasar spectrum had therefore to be subtracted from the off-nuclear spectrum to reveal the spectrum of the underlying host, but the extra noise and systematic errors introduced by this process severely limited the quality of the final spectra.

Thus, the main obstacles in these previous attempts to classify the hosts of powerful AGN were the difficulty in separating the underlying starlight from the glare of the quasar and - less immediately, but still of some importance - the lack of well-defined samples of a sufficient size to carry out straightforward statistical comparisons.

As far as possible, the design of the current study was intended to circumvent both these problems with the goal of obtaining clean spectra of the stellar component of radio-loud and radio-quiet quasar hosts and radio galaxies, which could then be used to search for systematic differences and similarities between the stellar populations and of the galaxies hosting each type of activity. Despite that fact that the radio galaxies lack bright nuclear point sources we were careful to adopt exactly the same observing strategy as used for the quasars to ensure that the data would be directly comparable.

In this paper we describe the observations and present the spectra. A second paper (Nolan et al. 2000) will describe the results of spectrophotometric modelling to estimate the ages and starformation histories of the galaxies (preliminary results have already been reported by Kukula et al. 1997). The current paper is organised as follows. Section 2 describes the samples used and Section 3 details the observing and data reduction strategies chosen to optimise the amount of starlight collected by the various instruments employed throughout the study. Section 4 gives an overview of the data obtained and Sections 5 and 6 contain more detailed information on the individual spectra.

2 SAMPLE SELECTION

Dunlop et al. (1993) and Taylor et al. (1996) observed a sample of intermediate-redshift ($0.1 \leq z \leq 0.3$) radio-loud and -quiet quasars[†] and Fanaroff-Riley Type II radio galaxies (RGs) in the near infrared (*K*-band: $2.2\mu\text{m}$) in order to compare the luminosities and morphologies of the galaxies associated with these three main types of powerful active nucleus. The choice of waveband was informed by the low quasar:host ratio in the near infrared, which allowed accurate determination of the galaxy properties from the ground with the minimum amount of confusion from the point spread function of the central quasar. Their sample was carefully constructed to ensure that the different types of object could be compared directly with one another: the radio-loud and -quiet quasars both have the same distribution of optical luminosities ($-23 \geq M_V \geq -26$) and both the radio-loud quasars and the radio galaxies have similar extended radio luminosities and morphologies and steep radio spectra. The sample is therefore ideal for investigating the influence of galaxy properties on the ‘radio loudness’ of

[†] Dunlop et al. define ‘radio quiet’ objects as those with $L_{5\text{GHz}} < 10^{24} \text{W Hz}^{-1} \text{sr}^{-1}$.

otherwise very similar quasars, and also for testing unified models of RLQs and RGs which predict that the properties of their hosts should be identical. A substantial subset of the sample has also formed the basis for an *R*-band imaging study using HST (Kukula et al. 1999, McLure et al. 1999, Dunlop et al. 2000), in which the enhanced angular resolution of HST has allowed both unambiguous identification of the host morphology and identification of detailed substructure in the quasar hosts and radio galaxies.

This sample provides an ideal starting point for a spectroscopic study of host galaxies because, in addition to the careful selection criteria, the existence of deep near-infrared images of every object provides us with a unique opportunity to minimise the contamination of the galaxy spectra by quasar light. Armed with knowledge of the extent and orientation of the host galaxy on the sky one is able to choose a slit position which is far enough from the nucleus to avoid the worst excesses of scattered quasar light, but which simultaneously maximises the amount of galaxy light falling onto the slit.

Out of the the 40 objects in the original Taylor et al. sample a total of 26 objects were observed in the current study (9 RQQs, 10 RLQs and 7 RGs). Details are listed in Table 1. Note that the radio source 3C59 has been shown by Meurs & Unger (1991) to consist of three separate sources, of which only the weakest appears to be associated with the quasar 0204+292. As a result, the radio luminosity of 0204+292 places it below our dividing line of $L_{5GHz} = 10^{24} \text{W Hz}^{-1} \text{sr}^{-1}$ and we classify it as an RQQ.

3 OBSERVATIONS

In order to assess the feasibility of our observing strategy initial observations of 11 of the nearest and brightest objects in the sample were carried out using the Mayall 4-m Telescope at Kitt Peak National Observatory. This was followed by a larger programme of observations using the 4.2-m William Herschel Telescope (WHT), part of the Isaac Newton Group of telescopes on La Palma.

Tables 2 and 3 list the observations made on the Mayall 4-m Telescope and the WHT respectively. Six objects (0054+144, 0157+001, 0736+017, 2141+279, 2247+140 and 2344+184) were observed with both telescopes in order to provide a check for consistency between the two sets of observations. The spectra for these objects are discussed in more detail in Section 6.

3.1 The Mayall 4-m Telescope

Observations of 11 objects were carried out with the R. C. Spectrograph on the Mayall 4-m Telescope at Kitt Peak in 1992 September and 1993 March (Table 1). The long-slit spectrograph uses a Tektronix 2048 × 2048 chip with 24- μm pixels, designated T2KB. The slit width was set to 3'' and the instrument was configured to give a spectral resolution of 1.9Å/pixel and a spatial resolution of 0.69''/pixel.

The slit was first centred on the quasar (or, if the object was a radio galaxy, on the galaxy centroid), before being rotated and offset to the desired position, usually 5 arcseconds off-nucleus.

To allow the removal of cosmic rays five 1800-second off-nuclear exposures were obtained for each object, along with a shorter exposure of the quasar itself. The spectra typically spanned wavelengths from 3500Å to 6000Å, although the precise range varied from object to object according to redshift; details for individual objects are given in Table 2. Data reduction was carried out using standard IRAF routines.

3.2 Observations with ISIS on the WHT

After the two runs at Kitt Peak had demonstrated that galaxy light could indeed be separated from that of the quasar and that useful spectra could be obtained, further observations were made of 22 objects (6 of which had already been observed at Kitt Peak) with the Intermediate Dispersion Spectroscopic and Imaging System (ISIS) at the 4.2 m William Herschel Telescope (WHT) on La Palma. ISIS uses a dichroic mirror to split the incoming light into red and blue beams which are then treated separately in spectrographs which have been optimised for the appropriate wavelength ranges (3000 → 6000Å for the blue arm and 5000 → 10000Å for the red). This arrangement allows a larger wavelength coverage than is possible with the single spectrograph on the Mayall 4-m, enabling us to extend our spectra further into the red and thus giving greater scope for constraining models of spectrophotometric evolution.

The data were obtained in four separate observing runs in 1993 November, 1994 May, 1994 September and 1995 March. The instrumental set-up differed slightly between the runs, resulting in variations in the wavelength ranges obtained. For the two sessions in 1994 the detectors in both the blue and red arms were Tektronix ('Tek') CCDs, with 24- μm pixels. In November 1993 and March 1996 the Tektronix chip in the red arm was replaced by an EEV P88300 chip, with 22.5- μm pixels, which allowed a slightly larger wavelength coverage. R158 gratings were used in each arm, giving a spectral resolution of 2.88Å pixel⁻¹ for the blue Tek chip and 2.90 (Tek) or 2.72Å pixel⁻¹ (EEV) for the red chips.

As with the observations at Kitt Peak the slit was first centred on the quasar nucleus, or the optical peak of the radio galaxy, and then offset to the desired position, 5'' from the quasar, and rotated to be at right angles to the direction of the offset. The slit width was set to 2'', placing the inner edge of the slit at least 4'' from the quasar position.

Once again exposures were limited to 1800 seconds duration. Whenever possible we aimed to obtain five such frames per object, giving a total on-source exposure time of 2.5 hours. On-nuclear quasar spectra were also taken when time permitted. Data reduction was carried out using the FIGARO package, part of the Starlink suite of astronomical software.

3.2.1 Calibration and splicing of red and blue spectra

The galaxies observed with the WHT tend to be fainter and/or at greater redshifts than those observed on the Mayall 4-m at Kitt Peak, and so additional care needed to be taken during the reduction of the WHT spectra. In particular, the procedure employed to optimize the extraction of the off-nuclear spectrum from the CCD frame means that

Table 1. Objects discussed in the current paper. Column 6 lists the telescope with which the object’s spectrum was obtained: M4M denotes the Mayall 4-m Telescope at Kitt Peak; WHT denotes the 4.2-m William Herschel Telescope on La Palma.

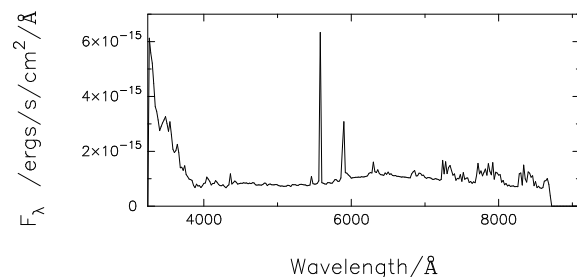
IAU name	Optical position (J2000)		V	z	Telescope	Alternative names
	RA (<i>h m s</i>)	Dec ($^{\circ}$ <i>'</i> <i>''</i>)				
<i>Radio-Quiet Quasars</i>						
0007+106	00 10 30.98	+10 58 28.4	15.40	0.089	M4M	III Zw 2
0054+144	00 57 09.92	+14 46 11.0	15.71	0.171	M4M/WHT	PHL909
0157+001	01 59 49.72	+00 23 41.0	15.69	0.164	M4M/WHT	Mrk 1014
0204+292	02 07 02.16	+29 30 45.4	16.00	0.109	WHT	3C59
0244+194	02 47 41.22	+19 40 53.6	16.66	0.176	WHT	MS 02448+19
1549+203	15 52 02.28	+20 14 01.6	16.50	0.250	WHT	1E15498+203, LB906, MS 15498+20
1635+119	16 37 46.54	+11 49 49.8	16.50	0.146	WHT	MC1635+119, MC 2
2215-037	22 17 47.35	-03 32 48.4	17.20	0.241	WHT	MS 22152-03, EX2215-037
2344+184	23 47 25.71	+18 44 58.4	15.90	0.138	M4M/WHT	E2344+184
<i>Radio-Loud Quasars</i>						
0137+012	01 39 57.24	+01 31 46.8	17.07	0.258	M4M	PHL1093
0736+017	07 39 18.01	+01 37 04.6	16.47	0.191	M4M/WHT	S0736+01, OI061
1004+130	10 07 26.12	+12 48 56.4	15.15	0.240	WHT	S1004+13, OL107.7, 4C13.41
1020-103	10 22 32.79	-10 37 44.2	16.11	0.197	M4M	S1020-103, OL133
1217+023	12 20 11.90	+02 03 42.3	16.53	0.240	WHT	S1217+02, UM492
2135-147	21 37 45.24	-14 32 55.6	15.53	0.200	WHT	S2135-14, PHL1657
2141+175	21 43 35.56	+17 43 49.1	15.73	0.213	WHT	OX169
2201+315	22 03 15.00	+31 45 38.3	15.58	0.298	M4M	B2 2201+31A, 4C31.63
2247+140	22 50 25.40	+14 19 49.9	15.33	0.237	M4M/WHT	PKS2247+14, 4C14.82
2349-014	23 51 56.14	-01 09 12.8	15.33	0.173	WHT	PKS2349-01, PB5564
<i>Radio Galaxies</i>						
0230-027	02 32 43.14	-02 33 34.1	19.20	0.239	WHT	PKS0230-027
0345+337	03 48 46.9	+33 53 16	19.00	0.244	WHT	3C93.1
0917+459	09 21 08.95	+45 38 55.8	17.22	0.174	WHT	3C219.0
1215-033	12 17 55.3	-03 37 23	18.90	0.184	WHT	
1330+022	13 32 53.27	+02 00 45.0	18.27	0.215	M4M	3C287.1
1334+008	13 37 31.38	+00 35 29.0	19.00	0.299	WHT	
2141+279	21 44 11.66	+28 10 18.9	18.15	0.215	M4M/WHT	3C436

the final flux calibration is only relative and not absolute - comparisons with the absolute fluxes obtained on the Mayall 4-m are therefore not meaningful.

The use of the red and blue arms of ISIS, whilst extending the wavelength coverage significantly, also introduces its own special problems. The large wavelength range made available by ISIS means that the spectra are affected by several prominent atmospheric emission features (Figure 1) which must be removed. Of these the strongest are the two oxygen lines at 5577 and 6300Å, the sodium D line at 5890Å, and the series of OH bands at wavelengths > 6500Å. Sky lines were removed by fitting a third order polynomial to two empty strips of sky on either side of the target spectrum but the removal process sometimes left a residual imprint of these features and this constitutes a major source of noise in some of the fainter spectra in our sample. Where this is the case the affected regions are mentioned in the description of the individual spectrum.

A second problem involves the splicing together of the two spectra from the red and blue arms of the instrument to give continuous wavelength coverage from 3200Å to 9000Å.

The reflection and transmission responses of the ISIS dichroic cross at $\sim 6100\text{\AA}$ and the instrument settings were designed to ensure a large overlap between the wavelength coverages of the two arms so that the full reflec-

**Figure 1.** Sky spectrum obtained at the WHT in September 1994. For the fainter targets in the sample the process of sky subtraction often leads to residuals around the positions of strong sky emission features such as the two lines of neutral oxygen at 5577 and 6300Å, the sodium D line at 5890Å, and the series of OH bands at wavelengths > 6500Å.

tion/transmission curves could be followed in the blue and the red spectra respectively. However, the faintness of many of the spectra effectively causes the flux calibration to fail at the red end of the blue spectrum and the blue end of the red, producing an artificial ‘lump’ in the spliced spectrum at the crossover point (6100Å or 6050Å, depending on the

Table 2. Objects observed on the Mayall 4-m Telescope at Kitt Peak. The detector used was a Tek T2KB chip. Columns are as follows: (1) source name, listed in RA order; (2) type of spectrum, ‘G’ = off-nuclear (galaxy) spectrum, ‘N’ = nuclear spectrum; (3) redshift; (4) date of observation (dd/mm/yy); (5) average airmass during observation; (6) average seeing during observation (arcsec); (7) number and length (in seconds) of consecutive exposures; (8) slit width (set to 3'' throughout); (9) wavelength range determined by grating setting; (10) positional offset of slit centre from quasar/galaxy centroid, and PA of slit (measured East from North).

Source	Type	z	Date	Airmass	Seeing (")	Exposure (sec)	Slit width	λ -range (Å)	Slit offset & PA
<i>Radio-Quiet Quasars</i>									
0007+106	G	0.089	25/09/92	1.10	1.7	5×1800	3''	3665-7121	5''N, 90°
	N	0.089	25/09/92	1.13	1.6	1×1800	3''	3665-7121	zero offset
0054+144	G	0.171	26/09/92	1.19	1.8	6×1800	3''	3659-7121	3''S, 4''E, 15°
	N	0.171	26/09/92	1.60	1.6	1×900	3''	3659-7121	zero offset
0157+001	G	0.164	25/09/92	1.26	1.8	5×1800	3''	3662-7121	5''N, 90°
	N	0.164	25/09/92	1.55	1.9	1×1200	3''	3662-7121	zero offset
2344+184	G	0.138	24/09/92	1.05	1.9	5×1800	3''	3665-7124	5''E, 177°
	N	0.138	24/09/92	1.15	2.5	1×1800	3''	3662-7121	zero offset
<i>Radio-Loud Quasars</i>									
0137+012	G	0.258	24/09/92	1.34	2.0	5×1800	3''	3662-7121	5''E, 155°
	N	0.258	26/09/92	1.70	1.8	1×900	3''	3659-7121	zero offset
0736+017	G	0.191	19/03/93	1.20	2.9	5×1800	3''	3530-7004	5''S, 90°
	G	0.191	20/03/93	1.19	1.4	4×1800	3''	3530-7004	5''S, 90°
	N	0.191	19/03/93	1.40	3.1	1×900	3''	3530-6989	zero offset
	N	0.191	20/03/93	1.17	1.4	1×1200	3''	3530-6989	zero offset
1020−103	G	0.197	19/03/93	1.41	2.9	3×1800	3''	3530-7004	3.5''W, 3.5''N, 45°
	G	0.197	20/03/93	1.38	1.4	4×1800	3''	3530-7004	3.5''W, 3.5''N, 45°
	N	0.197	19/03/93	1.36	2.9	1×900	3''	3530-6989	zero offset
2201+315	G	0.298	25/09/92	1.09	1.8	5×1800	3''	3665-7121	5''N, 84°
	N	0.298	25/09/92	1.00	1.8	1×1800	3''	3665-7121	zero offset
2247+140	G	0.237	24/09/92	1.26	1.2	5×1800	3''	3665-7124	4''E, 3''S, 38.7°
	N	0.237	24/09/92	1.06	1.2	1×1800	3''	3665-7124	zero offset
<i>Radio Galaxies</i>									
1330+022	G	0.215	20/03/93	1.18	1.4	5×1800	3''	3548-7004	2.5''N, 2.5''E, 135°
	N	0.215	19/03/93	1.18	3.1	2×1800	3''	3548-7004	zero offset
2141+279	G	0.215	26/09/92	1.03	1.8	4×1800	3''	3542-7124	4''E, 0°
	N	0.215	26/09/92	1.13	1.6	4×1800	3''	3542-7124	zero offset

exact instrumental settings at the time of the observations - see column 8 in Table 3).

Accordingly, in plotting the WHT spectra in Figure 2 we have blanked out the data points for 100Å on either side of the join region and replaced them with an averaged bridging section. We have masked out this section of the data in all subsequent modelling due to its inherent unreliability (see Nolan et al. 2000).

Due to the luminosity of the quasars themselves the on-nuclear spectra obtained with the WHT do not suffer from this problem and the red and blue sections have been spliced together directly with no noticeable discontinuity in flux at the join.

4 RESULTS

The galaxy spectra themselves are displayed in Figure 2 along with nuclear spectra for the same object, where such are available. All the data have been smoothed to 10-Å bins, and the WHT data are displayed with the region linking the individual red and blue spectra blanked out as described above. The expected position of various stellar absorption

features, including the 4000Å break are indicated by dotted lines in the off-nuclear spectra and the wavelengths of redshifted [OIII]λ5007 and Hα are also marked.

4.1 Data quality

A cursory examination of Figure 2 is enough to show that the quality of the off-nuclear spectra varies considerably from object to object. In the two initial observing runs at Kitt Peak priority was given to nearby objects with bright, prominent host galaxies, and the eleven spectra obtained with the Mayall 4-m enjoy a high signal-to-noise ratio. By contrast, the objects observed in later runs on the WHT tend to have larger redshifts and the signal-to-noise in many of these spectra is correspondingly lower due to the rapid reduction in surface brightness and increase in galactocentric radius with z .

4.2 Degree of quasar contamination

The primary goal of the observing program - to obtain spectra from the stellar component of the host whilst avoiding scattered emission from the active nucleus - appears to

Table 3. Galaxies observed with ISIS on the 4.2 m William Herschel Telescope on La Palma. Unlike the observations at Kitt Peak, nuclear spectra were not obtained for all objects observed with the WHT. Where such spectra are available, either from Kitt Peak or WHT observations, they are listed here and displayed in Figure 2 along with the off-nuclear (galaxy) spectrum. ‘M4M’ denotes that the nuclear spectrum was taken with the Mayall 4-m Telescope at Kitt Peak and ‘WHT’ that the spectrum was obtained using ISIS on the William Herschel Telescope. Columns are as follows: (1) source name, listed in RA order; (2) type of spectrum, ‘G’ = off-nuclear (galaxy) spectrum, ‘N’ = nuclear spectrum; (3) redshift; (4) date of observation (dd/mm/yy); (5) average airmass during integration period; (6) average seeing during observations (arcsec); (7) number and length (in seconds) of consecutive exposures; (8) slit width (2'' for all data except the six nuclear spectra obtained at Kitt Peak); (9) wavelength range determined by grating settings; (10) ‘join’ wavelength at which red and blue spectra have been spliced together; (11) positional offset of slit centre from quasar/galaxy centroid and PA of slit (measured East from North).

Source	Type	z	Date	Airmass	Seeing ($''$)	Exposure (sec)	Slit width	λ -range (\AA)	λ join (\AA)	Slit offset & PA
<i>Radio-Quiet Quasars</i>										
0054+144	G	0.171	01/09/94	1.30	0.9	4×1800	2''	3240-8700	6050	3.5''N, 4''W, 228°
	N(M4M)	0.171	26/09/92	1.60	1.6	1×900	3''	3659-7121	–	zero offset
0157+001	G	0.164	16/11/93	1.15	1.6	4×1800	2''	3456-9060	6100	5''N, 107.5°
	N(M4M)	0.164	25/09/92	1.55	1.9	1×1200	3''	3662-7121	–	zero offset
0204+292	G	0.109	17/11/93	1.03	1.0	5×1800	2''	3456-9060	6100	4.5''W, 0°
0244+194	G	0.176	02/09/94	1.06	1.7	4×1800	2''	3240-8700	6050	5''W, 180°
1549+203	G	0.250	30/03/95	1.05	1.2	4×1800	2''	3450-8991	6100	4''W, 3''N, 228°
1635+119	G	0.146	13/05/94	1.12	1.3	5×1800	2''	3240-8700	6050	4.75''W, 1''S, 172°
2215-037	G	0.241	01/09/94	1.60	0.9	3×1800	2''	3240-8700	6050	4.25''W, 3''N, 210°
2344+184	G	0.138	02/09/94	1.20	1.6	4×1800	2''	3240-8700	6050	3''N, 4''W, 215°
	N(M4M)	0.138	24/09/92	1.15	2.5	1×1800	3''	3662-7121	–	zero offset
<i>Radio-Loud Quasars</i>										
0736+017	G	0.191	16/11/93	1.14	1.0	5×1800	2''	3456-9060	6100	3.5''S, 3.5''W, 135°
	N(M4M)	0.191	19/03/93	1.40	3.1	1×900	3''	3530-6989	–	zero offset
1004+130	G	0.240	30/03/95	1.20	1.5	4×1800	2''	3450-8991	6100	3.5''N, 3.5''W, 43°
1217+023	G	0.240	11/05/94	1.20	0.8	4×1800	2''	3240-8700	6050	4''E, 3''N, 334°
2135-147	G	0.200	02/09/94	1.60	1.2	4×1800	2''	3240-8700	6050	3.5''W, 3.5''S, 315°
2141+175	G	0.213	13/05/94	1.60	1.0	3×1800	2''	3240-8700	6050	5''N, 290°
	N(WHT)	0.213	13/05/94	1.30	1.1	1×900	2''	3240-8700	6050	zero offset
2247+140	G	0.237	16/11/93	1.04	1.6	2×1800	2''	3456-9060	6100	4''E, 3''S, 38.7°
	N(M4M)	0.237	24/09/92	1.06	1.2	1×1800	3''	3665-7124	–	zero offset
2349-014	G	0.173	04/09/94	1.35	0.7	4×1800	2''	3240-8700	6050	1''S, 5''W, 324°
<i>Radio Galaxies</i>										
0230-027	G	0.239	02/09/94	1.30	2.0	2×1800	2''	3240-8700	6050	3.5''S, 3.5''W, 320°
	N(WHT)	0.239	01/09/94	1.20	1.5	1×1800	2''	3240-8700	6050	zero offset
0345+337	G	0.244	02/09/94	1.30	3.0	4×1800	2''	3240-8700	6050	5''N, 0.5''W, 265°
0917+459	G	0.174	19/11/93	1.10	1.7	5×1800	2''	3456-9060	6100	5''N, 90°
1215-033	G	0.184	13/05/94	1.19	0.9	3×1800	2''	3240-8700	6050	4''S, 3''E, 50°
1334+008	G	0.299	30/03/95	1.60	2.0	2×1800	2''	3450-8991	6100	3.5''W, 3.5''S, 135°
2141+279	G	0.215	02/09/94	1.20	1.0	4×1800	2''	3240-8700	6050	4.5''N, 2''E, 296°
	N(M4M)	0.215	26/09/92	1.13	1.6	4×1800	3''	3542-7124	–	zero offset

have been satisfied to a large extent. This can be demonstrated most easily by comparing the off-nuclear (galaxy) and nuclear spectra for the same object in Figure 2. The quasar spectra show prominent broad lines, notably those of $H\alpha$ $\lambda 6563$ and $H\beta$ $\lambda 4861$, with an increase in flux towards shorter wavelengths (particularly when the ‘blue bump’ continuum feature begins to emerge at $\lambda_{rest} \leq 5000\text{\AA}$).

Whilst emission lines do occur in the off-nuclear spectra, they tend to be relatively narrow forbidden lines such as $[\text{OIII}]\lambda\lambda 4363, 4959, 5007$. Where permitted lines occur, they lack the extremely broad profiles seen in the quasar nuclei, and are thus unlikely to result from scattering-induced contamination by nuclear light. In many cases the line ratios in the off-nuclear spectra also differ from those measured in

the quasars, indicating that the emission arises under different conditions than those prevailing in the active nucleus.

However, in spectra obtained under conditions of poor seeing, there is likely to be some degree of nuclear contamination and this will be exacerbated if the object was observed far from the zenith, where differential atmospheric refraction may also lead to significantly more contamination at the blue end of our wavelength range than in the red. Although the extent of such contamination is difficult to measure directly, Tables 2 and 3 list the atmospheric seeing and airmass at the time each spectrum was obtained, to allow a rough assessment of the problem to be made.

Table 4. Strength of the 4000Å break feature in the host galaxy spectra (defined as the ratio of the flux density between 4050 and 4250Å to that between 3750 and 3950Å in the object’s rest frame, and measured in terms of F_ν). M4M denotes the Mayall 4-m Telescope at Kitt Peak; WHT denotes the 4.2-m William Herschel Telescope on La Palma. 3-sigma errors were estimated from the scatter in the flux density across the two reference regions.

IAU name	Telescope	Break strength
<i>Radio-Quiet Quasars</i>		
0007+106	M4M	1.4 ± 0.1
0054+144	M4M	1.3 ± 0.1
	WHT	1.3 ± 0.1
0157+001	M4M	1.3 ± 0.1
	WHT	1.3 ± 0.1
0204+292	WHT	1.6 ± 0.1
0244+194	WHT	0.8 ± 0.2
1549+203	WHT	2.0 ± 0.1
1635+119	WHT	1.7 ± 0.1
2215-037	WHT	1.4 ± 0.1
2344+184	M4M	1.7 ± 0.1
	WHT	1.4 ± 0.1
<i>Radio-Loud Quasars</i>		
0137+012	M4M	1.7 ± 0.1
0736+017	M4M	1.4 ± 0.1
	WHT	1.8 ± 0.1
1004+130	WHT	1.1 ± 0.1
1020-103	M4M	1.7 ± 0.1
1217+023	WHT	1.1 ± 0.1
2135-147	WHT	2.0 ± 0.3
2141+175	WHT	0.9 ± 0.2
2201+315	M4M	1.4 ± 0.1
2247+140	M4M	1.9 ± 0.1
	WHT	2.0 ± 0.1
2349-014	WHT	1.5 ± 0.1
<i>Radio Galaxies</i>		
0230-027	WHT	1.9 ± 0.4
0345+337	WHT	1.7 ± 0.4
0917+459	WHT	2.0 ± 0.1
1215-033	WHT	1.9 ± 0.2
1330+022	M4M	1.6 ± 0.1
1334+008	WHT	1.1 ± 0.2
2141+279	M4M	2.2 ± 0.1
	WHT	1.3 ± 0.2

4.3 Spectral features

The characteristic shape of the stellar continuum, including features such as the 4000Å break and various stellar absorption lines, is easily recognisable in most cases. The 4000Å break is particularly important for comparison between data and models of the stellar population. Since it covers a large wavelength interval it is relatively insensitive to the effects of instrument resolution and noise (Hamilton 1985). The break amplitude (defined as the ratio of the average flux density between rest-frame 4050 and 4250Å to that between 3750 and 3950Å) is therefore widely used as a tracer of spectral evolution (eg Bruzual 1983). The discontinuity results from the combined effect, shortwards of 4000Å, of lines of several elements heavier than helium, in a variety

of ionization states, along with the crowding of higher order Balmer lines. If a significant population of massive young stars is present the enhanced degree of ionization causes the feature to weaken; it is most prominent in the spectrum of a well-established stellar population in which the most massive stars have had time to evolve away from the main sequence. Hence the 4000Å break is sensitive to both spectral type and metallicity, although if we assume a constant metallicity (a reasonable assumption for a particular galaxy at a fixed radius) it becomes a good indicator of the mean age of the local stellar population. The strength of this feature, as measured in each of the current spectra, is listed in Table 4. Other stellar absorption features, such as G band (4300 to 4320Å) and the Mg Ib (5173Å) and Feλ5270 lines, are also clearly present in many of the spectra.

Several of the off-nuclear spectra (eg 0054+144, 2201+315), despite showing a clear break at 4000Å and a continuum longwards of this wavelength which can be fitted extremely well by a passively ageing stellar population (Nolan et al. 2000), also display a contribution from a component which rises steeply towards the blue. The slope of this feature closely resembles that of a quasar SED, and its presence is often (but not always) accompanied by emission lines characteristic of quasar nuclei, suggesting that it is in fact scattered light from the quasar itself, the result either of atmospheric scattering or (since the feature is not always correlated with poor observing conditions) of scattering within the ISM of the host galaxy. Another possibility is that the blue excess indicates the presence of a substantial population of young stars within the host galaxy. If this latter case were true then it would pose a serious problem for the unification of RLQs and RGs since none of the radio galaxies display such a component. The issue of excess blue continuum is raised on a case-by-case basis in the following section, but a full discussion in the light of detailed stellar population synthesis modelling is deferred to the companion paper by Nolan et al. (2000).

The average values of the 4000Å break strength for the three types of object in the sample are 1.4 (RQQ hosts), 1.5 (RLQ hosts) and 1.7 (RGs). These are all somewhat lower than the value of ~ 2.0 measured for local inactive elliptical galaxies by Hamilton (1985), but we note that there is a wide scatter in our sample and that the lowest values are all associated either with spectra in which the signal to noise is particularly poor (eg 0244+292, 1004+130, 1334+008) or those which clearly show an extra source of continuum emission at short wavelengths (eg the quasars 0054+144, 1217+023, 2141+175). The cleanest spectra generally have break strengths which are consistent with those seen in ‘normal’ well-established galaxies.

As a final caveat we note that these spectra tell us only about the stellar composition of the region of the galaxy covered by the slit - we cannot, for example, rule out the presence of a significantly different stellar population closer to the nucleus, or concentrated in clumps which the slit happens to avoid. However, the slit has a width of at least 2 arcsec and, as can be seen from the contour plots in Figure 2, its length cuts across a significant fraction of the galaxy in the transverse direction. The area covered often amounts to several square arcseconds (equivalent to several tens of square kiloparsecs at typical redshifts) and therefore represents a good general sample of the outer regions of the host.

5 INDIVIDUAL OBJECTS

Objects are listed under their IAU names (alternative names are listed in Table 1), in order of increasing right ascension. The classification of each object as either an RQQ, an RLQ or a radio galaxy is indicated in parentheses, along with the name(s) of the telescope(s) on which off-nuclear spectra were obtained. The form of the spectrum is described, noting any peculiar features as well as the presence or otherwise of a 4000Å break at the expected observed wavelength (λ_{obs}). We also note the morphology of the galaxy (disc or elliptical) based on its surface brightness profile in the *K* or *R*-band continuum images by Taylor et al. (1996) (*K*-band; UKIRT) or McLure et al. (1999) and Dunlop et al. (2000) (*R*-band; HST). For a more detailed description of previous imaging studies of the host galaxies see Dunlop et al. (1993) (RLQs and RQQs) or Taylor et al. (1996) (RGs).

0007+106 (RQQ; M4M): the nuclear spectrum of this radio-quiet quasar shows prominent broad $H\alpha\lambda 6583$ and $H\beta\lambda 4861$ emission as well as narrower forbidden line emission from species including [OIII] and [FeVII]. The off-nuclear spectrum of the host galaxy has a high signal-to-noise and displays little sign of contamination from the quasar: the contribution from emission lines is very small, and the 4000Å break is clearly visible (redshifted to 4356Å) despite the rapid increase in quasar flux towards the blue end of the spectrum, which would tend to mask the break if scattering were significant. G band and Mg Ib absorption are also present. We note that the slit crosses the optical arc-like structure to the north of the quasar which Hutchings et al. (1984) suggest may be a spiral arm. Previous spectroscopy of this region by Green, Williams & Morton (1978) showed narrow emission lines (with different line ratios from those in the nucleus) and a red continuum which they attribute to starlight. However, this region only constitutes a small fraction of the galaxy light intercepted by the slit in the current observations. Taylor et al. (1996) find that an exponential disc profile provides a good fit to the NIR surface brightness distribution of the galaxy. (Morphology: disc; Taylor et al. 1996.)

0054+144 (RQQ; M4M & WHT): quasar continuum emission dominates the nuclear spectrum of this RQQ, although $H\beta\lambda 4861$ and [OIII] $\lambda\lambda 4363, 4959, 5007$ lines are visible. These lines are not prominent in either the Mayall 4-m or WHT off-nuclear spectra of the host (particularly the latter spectrum) but bluewards of the (relatively weak) 4000Å break (at $\lambda_{obs} = 4684\text{Å}$) the galaxy spectrum displays a marked increase in flux, very similar in form to that displayed by the quasar itself. This component is seen in both off-nuclear spectra, which were taken at different times, under different seeing conditions, and used different slit positions, so it is not clear whether we are seeing quasar light which is being scattered into our line of sight either by the atmosphere or by the interstellar medium of the host galaxy, or whether the blue excess is due to a population of young stars. G band, Mg Ib and Fe5270 absorption features appear in the Mayall 4-m spectrum. McLure et al. (1999) classify the galaxy as an elliptical: its light profile is very well described by an $r^{1/4}$ law and the galaxy itself is quite red ($R - K = 3.14$), but a tidal interaction with a nearby companion is suggested by the extension to the NW of the nu-

cleus (Dunlop et al. 1993). (Morphology: elliptical; McLure et al. 1999.)

0137+012 (RLQ; M4M): the 4000Å break in this object is quite clear (at $\lambda_{obs} = 5032\text{Å}$) and there is little evidence of nuclear emission lines. (Morphology: elliptical; McLure et al. 1999.)

0157+001 (RQQ; M4M & WHT): the off-nuclear spectrum obtained with the Mayall 4-m does not appear to be strongly contaminated by emission from the nucleus and the 4000Å break is visible at $\lambda_{obs} = 4656\text{Å}$. The G band absorption feature is also present. However, in the spectrum taken with the WHT using a similar slit position, there appears to be a significant contribution from the quasar continuum bluewards of the break. The signal:noise ratio in the WHT spectrum is much reduced longwards of 7500Å due to residuals from the subtracted OH bands. In both cases the slit intercepts the prominent tidal arm which extends north and NW of the nucleus (MacKenty & Stockton 1984) and is known to contain several emission line regions (Stockton & MacKenty 1987), although emission lines are not strongly evident in the integrated spectra presented here. Previous spectroscopy of this structure by Heckman et al. (1984) showed a velocity difference of $300 \pm 200 \text{ km s}^{-1}$ between the arm and the quasar itself. McLure et al. (1999) find that the underlying smooth *R*-band continuum light is well described by an $r^{1/4}$ -law, though conceivably this might be another result of the tidal interaction. (Morphology: elliptical; McLure et al. 1999.)

0204+292 (RQQ; WHT): the 4000Å break ($\lambda_{obs} = 4436\text{Å}$) is quite strong in this WHT spectrum, but residuals from oxygen and OH features from the sky spectrum are also present. (Morphology: disc; Taylor et al. 1996)

0230-027 (RG; WHT): the off-nuclear spectrum of this small, faint radio galaxy suffers from low signal to noise and residual sky features are visible. However a break can be seen at $\lambda_{obs} = 4952\text{Å}$. The nuclear spectrum of this object is also dominated by starlight, although narrow emission lines are present. (Morphology: elliptical; Dunlop et al. 2000.)

0244+194 (RQQ; WHT): the signal to noise in this off-nuclear spectrum is very low. Apart from residual sky features there is some evidence for a drop in the continuum level around $\lambda_{obs} = 4704\text{Å}$ (the expected position of the 4000Å break), but also for a blue component shortwards of this, perhaps indicative of nuclear contamination. (Morphology: elliptical; McLure et al. 1999.)

0345+337 (RG; WHT): the spectrum is noisy, but a break feature appears to be present at $\lambda_{obs} = 4936\text{Å}$. The WHT slit intercepts a bright knot NW of the quasar which Taylor et al. (1996) suggest may be an embedded companion galaxy. (Morphology: elliptical; McLure et al. 1999.)

0736+017 (RLQ; M4M & WHT): the WHT spectrum, though noisier and suffering from OH-band residuals at long wavelengths, agrees well with the spectrum obtained previously at Kitt Peak. The 4000Å break is quite clear at $\lambda_{obs} = 4764\text{Å}$ and weak [OIII], $H\alpha$ and $H\beta$ features can also be seen, though they appear to be narrower than those in the nuclear spectrum. The galaxy itself is highly disturbed, but McLure et al. (1999) fit an $r^{1/4}$ -law profile to the smooth component of the *R*-band continuum. (Morphology: elliptical; McLure et al. 1999.)

0917+459 (RG; WHT): the off-nuclear spectrum is pure stellar continuum, with a strong break at $\lambda_{obs} = 4696\text{Å}$.

The galaxy isophotes are complex but McLure et al. (1999) find the underlying distribution to be well described by an $r^{1/4}$ -law. (Morphology: elliptical; McLure et al. 1999.)

1004+130 (RLQ; WHT): OH-band residuals are the only prominent feature of this off-nuclear spectrum, with little evidence for either emission lines or a 4000Å break (at $\lambda_{obs} = 4960\text{Å}$). The absence of a strong break may reflect the fact that the elliptical host galaxy of this quasar is known to possess unusual ‘spiral’ features close to the nucleus (McLure et al. 1999), perhaps indicating the presence of a significant population of young stars. Stockton & MacKenty (1987) note that there is no significant extended [OIII] emission in this object. (Morphology: elliptical; McLure et al. 1999.)

1020–103 (RLQ; M4M): despite the presence of stellar absorption features such as G band and a 4000Å break at $\lambda_{obs} = 4788\text{Å}$, the off-nuclear spectrum also contains many emission lines as well as a blue excess, which may indicate a significant contribution from scattered quasar light (the seeing was quite poor for much of the observations). Dunlop et al. (1993) note that the quasar is off-centre and that the galaxy isophotes appear to be swept back towards the SW, providing evidence for disturbance in this object. (Morphology: elliptical; Dunlop et al. 1999.)

1215–033 (RG; WHT): this spectrum displays only a weak break at $\lambda_{obs} = 4736\text{Å}$. OH-band residuals dominate longwards of 7500Å. (Morphology: elliptical; Dunlop et al. 2000.)

1217+023 (RLQ; WHT): a weak break feature is present at $\lambda_{obs} = 4960\text{Å}$ but shortwards of this the spectrum is dominated by a component which rises towards the blue possibly indicating scattered nuclear continuum (there is however little evidence for accompanying nuclear line emission, and the seeing during the observations was excellent). At the red end, poor subtraction of OH bands has reduced the signal to noise ratio of the spectrum. (Morphology: elliptical; Dunlop et al. 2000.)

1330+022 (RG; M4M): weak [OIII] lines occur in the off-nuclear spectrum of this radio galaxy and the stellar continuum shows G band absorption and a strong 4000Å break feature at $\lambda_{obs} = 4860\text{Å}$. By contrast, the nuclear spectrum shows evidence for broad $H\beta\lambda 4861$ and the less prominent break may indicate a contribution from a quasar-type continuum or perhaps a nuclear starburst region. (Morphology: elliptical; Dunlop et al. 2000.)

1334+008 (RG; WHT): a very noisy spectrum obtained under poor conditions, the underlying continuum is confused by many residual sky features. The apparent increase in flux shortwards of 4500Å almost certainly reflects a failure of the flux calibration at very low light levels. However, there is some evidence for a break at the expected wavelength of $\lambda_{obs} = 5196\text{Å}$. The slit intercepts one of the secondary nuclei reported by Taylor et al. (1996). (Morphology: elliptical; Taylor et al. 1996.)

1549+203 (RQQ; WHT): the extended nebulosity around this RQQ, though confused by a foreground galaxy cluster, shows a strong break feature at the expected wavelength of $\lambda_{obs} = 5000\text{Å}$ and little evidence for emission lines. OH-band residuals add to the noise levels at long wavelengths. (Morphology: elliptical; Dunlop et al. 2000.)

1635+119 (RQQ; WHT): the 4000Å break is clearly visible at $\lambda_{obs} = 4584\text{Å}$, but residual sky features degrade the

quality of the spectrum towards the red end. (Morphology: elliptical; McLure et al. 1999.)

2135–147 (RLQ; WHT): generally low signal to noise with prominent residuals due to sky features. However, there is weak evidence for a break at $\lambda_{obs} = 4800\text{Å}$. The galaxy appears to be disturbed and possesses a secondary nucleus to the SE of the quasar (Stockton 1982) which may also be active (Hickson & Hutchings 1987). The WHT slit intercepts a region to the SW of the quasar at which Stockton & MacKenty (1987) report extended [OIII] emission. Narrow $H\alpha$ is present in the current spectrum but the [OIII] lines fall within the join region where the signal is unreliable. (Morphology: elliptical; Dunlop et al. 2000.)

2141+175 (RLQ; WHT): low signal to noise and the presence of a strong blue component may serve to mask any evidence of a 4000Å break in this object (expected at $\lambda_{obs} = 4852\text{Å}$). The idea that this blue component originates as scattered quasar light is bolstered by the possible presence of the $H\alpha$ line, but the issue is confused by strong sky residuals (although the seeing was good, the airmass during the observations was relatively high, so differential refraction might explain the presence of quasar contamination at shorter wavelengths without requiring the presence of a strong $H\alpha$ line). The elongated appearance of the galaxy is apparently the result of an edge-on tidal arm consisting of old stars (Stockton & Farnham 1991). However, the WHT slit crosses the galaxy to the NE of the quasar, where the starlight appears to follow a bulge-dominated $r^{1/4}$ -law (McLure et al. 1999a). (Morphology: elliptical; McLure et al. 1999.)

2141+279 (RG; M4M & WHT): the off-nuclear spectrum taken at Kitt Peak shows a weak [OIII] $\lambda 5007$ line, a break feature at $\lambda_{obs} = 4860\text{Å}$ and Mg Ib absorption. The WHT spectrum is much noisier, but generally consistent with the features in the earlier data. The nuclear spectrum of this radio galaxy is also dominated by starlight, although prominent narrow lines are present. (Morphology: elliptical; McLure et al. 1999.)

2201+315 (RLQ; M4M): this object shows prominent G band absorption but only a weak 4000Å break at $\lambda_{obs} = 5192\text{Å}$, along with low-equivalent-width [OIII] lines. A blue component shortwards of the break is consistent with scattering of the nuclear quasar continuum. (Morphology: ambiguous; Taylor et al. 1996.)

2215–037 (RQQ; WHT): the spectrum is relatively noisy with prominent residuals from all the bright sky features. The apparent ‘hump’ at $\sim 6000\text{Å}$ is an artifact that results from the sodium D sky line coinciding with the beginning of the masking region that links the red and blue halves of the spectra from ISIS. There is little evidence for a prominent break at the expected wavelength of $\lambda_{obs} = 4964\text{Å}$. Both Hutchings et al. (1989) and McLure et al. (1999b) classify the galaxy as a non-interacting elliptical system. (Morphology: elliptical; Dunlop et al. 2000.)

2247+140 (RLQ; M4M & WHT): the galaxy’s 4000Å break is visible at $\lambda_{obs} = 4948\text{Å}$ in the Mayall 4-m spectrum, along with G band absorption. The data obtained on the WHT are consistent with this, although residual sky features from oxygen and sodium D lines and the OH bands are also present. (Morphology: elliptical; McLure et al. 1999.)

2344+184 (RQQ; M4M & WHT): both the Mayall 4-m

and WHT spectra show a break at $\lambda_{obs} = 4552\text{\AA}$ as well as G band absorption and are generally consistent with one another despite their differing slit positions. The nuclear spectrum of this object is also dominated by starlight; 2344+184 is one of the least powerful quasars in the current study and technically qualifies as a Type 1 Seyfert galaxy. The surface brightness profile is that of a disc galaxy, although a bulge dominates in the central regions (McLure et al. 1999) and there is also evidence for a bar (Hutchings, Janson & Neff 1989). (Morphology: disc; McLure et al. 1999.)

2349–014 (RLQ; WHT): there is a weak break feature at $\lambda_{obs} = 4692\text{\AA}$ and also evidence for weak H β , [OIII] λ 5007 and H α lines. The red end of the spectrum is dominated by residual atmospheric OH band emission. (Morphology: elliptical; McLure et al. 1999.)

6 COMPARISON OF MAYALL 4-M AND WHT RESULTS

Six objects in the current sample (the RQQs 0054+144, 0157+001 and 2344+184, the RLQs 0736+017 and 2247+140, and the radio galaxy 2141+279) were observed with both the Mayall 4-m Telescope and the WHT. This duplication allows us to check for systematic differences between the spectra obtained with each instrument and to this end the are replotted one above the other in Figure 3. Since the observations were often made under different atmospheric conditions they also provide a means of assessing the degree to which any contamination by nuclear light can be attributed to either the airmass and seeing conditions at the time of the observations or scattering within the host galaxy itself. Where a different slit position was used, the two spectra allow us to examine the degree of homogeneity in the stellar composition of the galaxy.

It should be noted that due to the optimization method used to extract the WHT spectra, their flux calibration can only be considered as relative, not absolute. Different slit widths were also used on the two instruments. Comparisons of the flux densities obtained on the two telescopes are therefore not meaningful.

0054+144 (RQQ): different slit positions were used for the Mayall 4-m and WHT observations. The spectrum obtained with the Mayall 4-m shows a contribution from H β /[OIII] at $\lambda_{obs} \sim 5800\text{\AA}$, which is lacking in the WHT data. However, the underlying continuum is very similar in both spectra and the measured depth of the (weak) 4000 \AA break is very similar in each. This implies that the emission lines detected in the Mayall 4-m spectrum are a local feature, produced *in situ* rather than being due to scattered light from emission-line regions in the nucleus, since they do not appear to be accompanied by a corresponding amount of scattered nuclear continuum. The consistency in the strength of the 4000 \AA break at the two observing epochs, along with its relative weakness, suggests the presence of a significant population of young stars in the host galaxy. McLure et al. (1999) report a tidal feature visible in their *R*-band HST image of the elliptical host galaxy which may be linked to the origin of this young stellar population.

0157+001 (RQQ): the slit positions used in the two sets of observations were essentially the same. However, the WHT spectrum shows excess blue continuum shortwards of this

feature. The two spectra were taken under what were ostensibly very similar atmospheric conditions, but we note that a very good approximation of the WHT spectrum can be obtained simply by adding a scaled version of the nuclear spectrum to the off-nuclear Mayall 4-m data. This suggests that atmospheric scattering is to blame for the blue excess in the WHT spectra.

0736+017 (RLQ): the two spectra were both taken under good atmospheric conditions and using the same slit position. The agreement between the two is excellent.

2141+279 (RG): the WHT spectrum has a much lower signal:noise ratio than the Mayall 4-m spectrum, and uses a different slit position. However, the overall continuum shape is in good agreement with the earlier data. Both slits intercept an extension to the NE of the nucleus which may be a tidal feature caused by interaction with a northern companion.

2247+140 (RLQ): the same slit position was used for both spectra, although the seeing during the WHT run was quite poor ($\sim 1.6''$). The two datasets are consistent with one another, with a relatively strong 4000 \AA break and little sign of an additional blue continuum component from either young stars or scattered quasar light.

2344+184 (RQQ): different slit positions were used on the two different instruments, and the WHT spectrum shows an excess of blue emission and a correspondingly weaker 4000 \AA break. The seeing conditions were actually worse during the M4M observations, making atmospheric scattering of quasar light an unlikely culprit. Moreover, we note that the nuclear spectrum of this low-luminosity quasar is not particularly blue and itself shows prominent stellar continuum features (see Figure 2). More likely is that the WHT slit crossed a region of the galaxy containing a large number of young stars. The host of 2344+184 is a disc galaxy, with a central bulge and prominent spiral arms (McLure et al. 1999). (Hutchings et al. (1989) also suggest the presence of a bar.)

7 SUMMARY

We describe and present optical spectra of 26 galaxies hosting powerful nuclear activity. The sample contains carefully matched subsamples of all three types of powerful AGN - radio-quiet and radio-loud quasars, and FRII radio galaxies - enabling us to investigate the relationship between the host galaxy and the radio properties of the resident AGN and also to test unified models for radio-loud objects.

The spectra were taken 5 arcsec *off-nucleus* and, via a careful choice of slit position, aim to maximise the amount of galaxy light entering the instrument whilst avoiding contamination from the active nucleus. In the majority of cases this approach appears to have been successful; the continuum is clearly overwhelmingly stellar in origin and even when the presence of scattered nuclear emission is suspected, features such as the 4000 \AA break are still clearly discernable. In almost all objects we detect at least some stellar signatures.

A second paper (Nolan et al. 2000) will discuss spectrophotometric modelling of the galaxy spectra in order to determine the ages and starformation histories of their constituent stellar populations.

ACKNOWLEDGMENTS

The authors would like to thank the staff at KPNO and the ING for their assistance during the observations, and the anonymous referee whose comments and suggestions resulted in several improvements in the final paper. DHH and MJK acknowledge PPARC support. This research has made use of the NASA/IPAC Extragalactic Database (NED), which is operated by the Jet Propulsion Laboratory, California Institute of Technology, under contract with the National Aeronautics and Space Administration.

REFERENCES

- Bahcall J. N., Kirhakos S. & Schneider D. P., 1994, *ApJ*, 435, L11
 Bahcall J. N., Kirhakos S. & Schneider D. P., 1995a, *ApJ*, 447, L1
 Bahcall J. N., Kirhakos S. & Schneider D. P., 1995b, *ApJ*, 450, 486
 Bahcall J. N., Kirhakos S. & Schneider D. P., 1996, *ApJ*, 457, 557
 Bahcall J. N., Kirhakos S., Schneider D. P., & Saxe D. H., 1997, *ApJ*, 479, 642
 Boroson T. A. & Oke J. B., 1982, *Nature*, 296, 397
 Boroson T. A., Oke J. B. & Green R. F., 1982, *ApJ*, 263, 32
 Boroson T. A. & Oke J. B., 1984, *ApJ*, 281, 535
 Boroson T. A., Persson S. E. & Oke J. B., 1985, *ApJ*, 293, 120
 Boyce P. J. et al., 1998, *MNRAS*, 298, 121
 Bruzual G., 1983, *ApJ*, 273, 105
 Disney M. J. et al., 1995, *Nature*, 376, 150
 Dunlop J. S., McLure R. J., Kukula M. J., Baum S. A., O’Dea C. P. & Hughes D. H., 2000, in preparation
 Dunlop J. S., Taylor G. L., Hughes D. H. & Robson E. I., 1993, *MNRAS*, 264, 455
 Green R. F., Williams T. B. & Morton D. C., 1978, *ApJ*, 226, 729
 Hamilton D., 1985, *ApJ*, 297, 371
 Heckman T. M., Bothun G. D., Balick B. & Smith E. P., 1984, *AJ*, 89, 958
 Hickson P. & Hutchings J. B., 1987, *ApJ*, 312, 518
 Hooper E. J., Impey C. D. & Foltz C. B., 1997, *ApJ*, 480, L95
 Hutchings J. B., Crampton D., Campbell B., Duncan D. & Glendenning B., 1984, *ApJS*, 55, 319
 Hutchings J. B. & Crampton D., 1990, *AJ*, 99, 37
 Hutchings J. B. et al., 1994, *ApJ*, 429, L1
 Hutchings J. B., Janson T. & Neff S. G., 1989, *ApJ*, 342, 660
 Hutchings J. B. & Morris S. C., 1995, *AJ*, 109, 1541
 Kukula M. J., Dunlop J. S., Hughes D. H., Taylor G. L. & Boroson T., 1997, in ‘Quasar Hosts’, eds. Clements D. L. & Pérez-Fournon I., Springer:Berlin, p. 177
 Kukula M. J., Dunlop J. S., McLure R. J., Baum S. A., O’Dea C. P. & Hughes D. H., 1999, *Advances In Space Research*, 23, 1131
 MacKenty J. W. & Stockton A., 1984, *ApJ*, 283, 64
 McHardy I. M., Merrifield M. R., Abraham R. G. & Crawford C. S., 1994, *MNRAS*, 268, 681
 McLeod K. K. & Rieke G. H., 1995a, *ApJ*, 441, 96
 McLeod K. K. & Rieke G. H., 1995b, *ApJ*, 454, L77
 McLeod K. K., Rieke G. H. & Storrie-Lombardi L., 1999, *ApJ*, 511, L67
 McLure R. J., Kukula M. J., Dunlop J. S., Baum S. A., O’Dea C. P. & Hughes D. H., 1999, *MNRAS*, 308, 377
 Meurs E. J. A. & Unger S. W., 1991, *A&A*, 252, 63
 Nolan L. A., Dunlop J. S., Kukula M. J., Hughes D. H., Boroson T., & Jimenez R., 2000, submitted to *MNRAS*
 Stockton A., 1982, *ApJ*, 257, 33
 Stockton A. & Farnham T., 1991, *ApJ*, 371, 525
 Stockton A. & MacKenty J. W., 1987, *ApJ*, 316, 584
 Taylor G. L., Dunlop J. S., Hughes D. H. & Robson E. I., 1996, *MNRAS*, 283, 930
 Urry C. M. & Padovani P., *PASP*, 107, 803
 Véron-Cetty M. -P. & Woltjer L., 1990, *A&A*, 236, 69

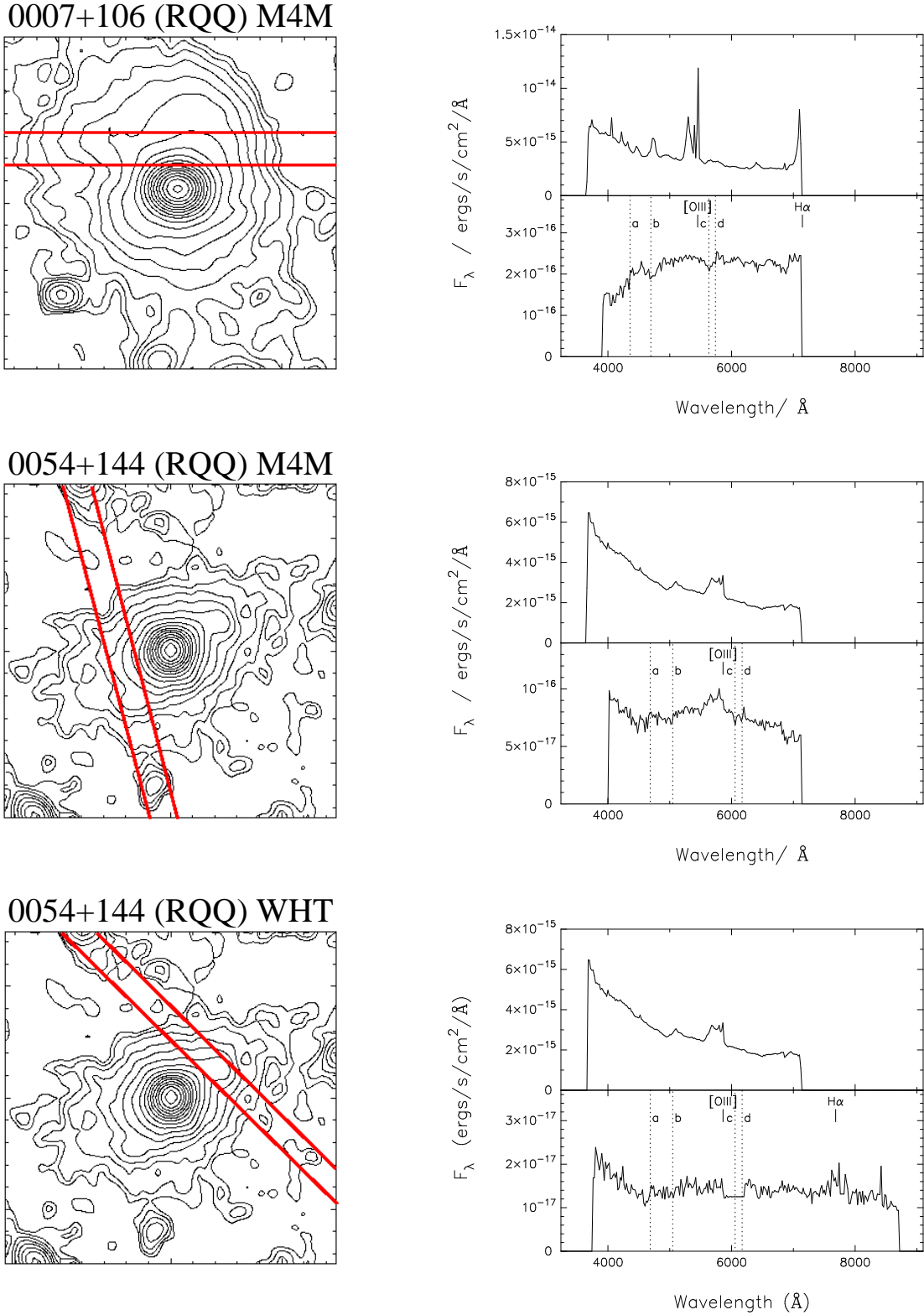
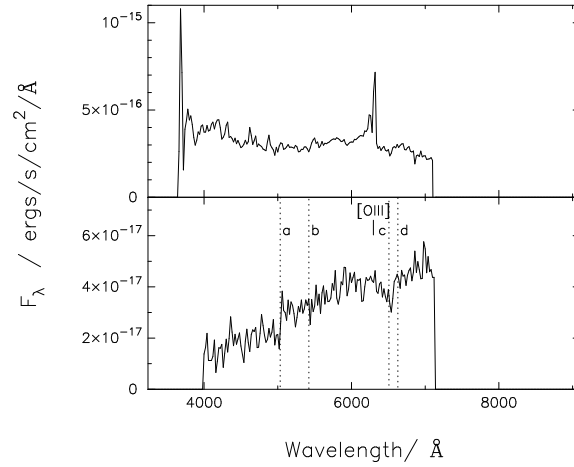
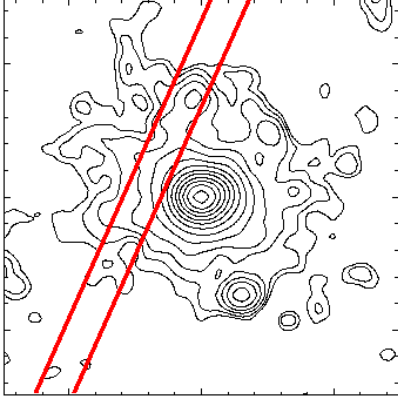
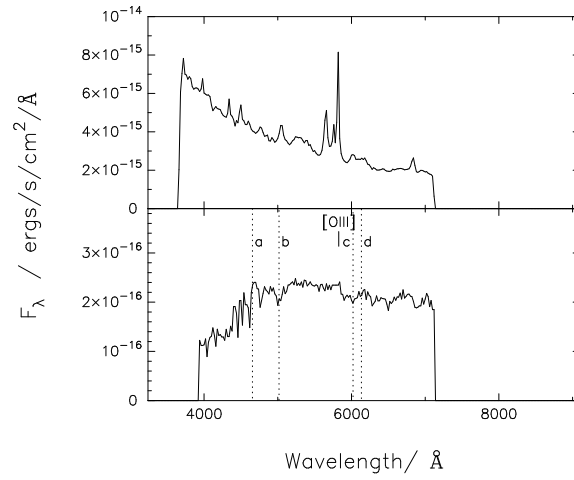
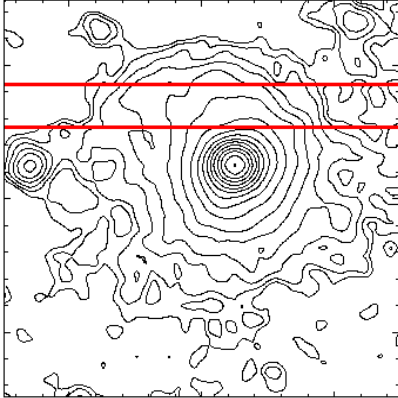


Figure 2. Spectra obtained on the Mayall 4-m Telescope (M4M) at Kitt Peak and the William Herschel Telescope (WHT) on La Palma, in order of increasing right ascension. The spectra are plotted at the observed wavelength in units of F_{λ} . In each case the lower panel shows the off-nuclear (host galaxy) spectrum and the upper panel the nuclear (quasar) spectrum where available. The expected positions of various stellar absorption features are marked by vertical dotted lines in the off-nuclear spectra: (a) the 4000Å break; (b) G band ($\lambda_{rest} = 4300 \rightarrow 4320\text{Å}$); (c) Mg Ib ($\lambda_{rest} = 5173\text{Å}$); (d) Fe λ 5270. The redshifted wavelengths of the [OIII] λ 5007 and H α emission lines are also indicated. The side panels show the slit position and orientation for the off-nuclear data superimposed on the near-infrared (2.2 μ m) contours of the object from Taylor et al. (1996) (each panel is 30×30 arcsec²).

0137+012 (RLQ) M4M



0157+001 (RQQ) M4M



0157+001 (RQQ) WHT

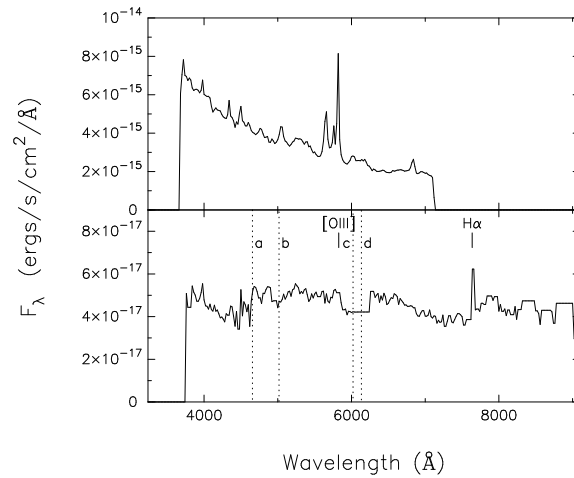
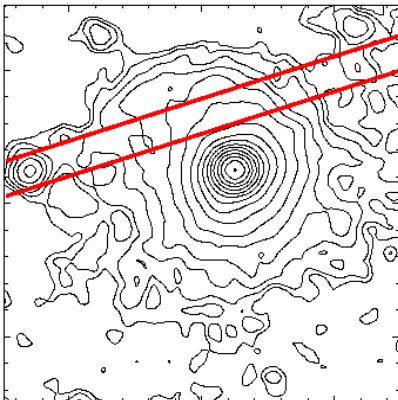
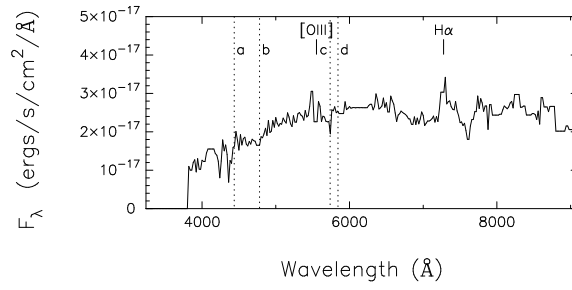
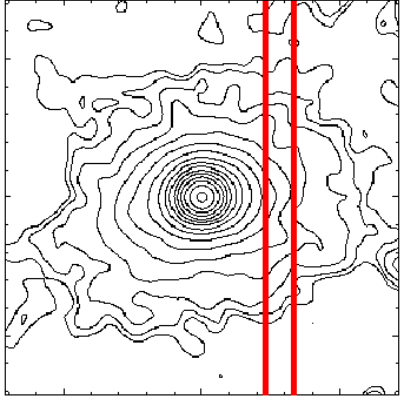
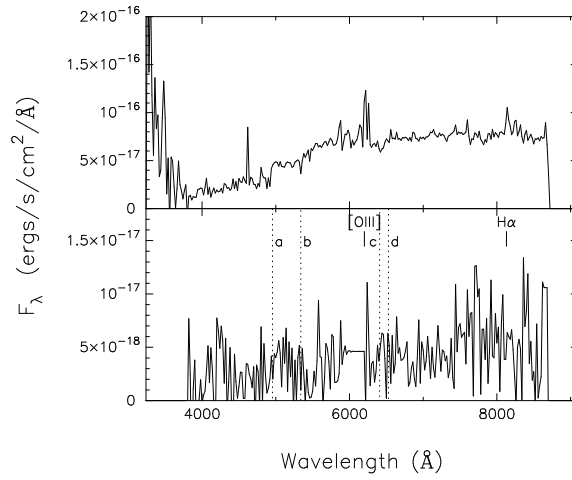
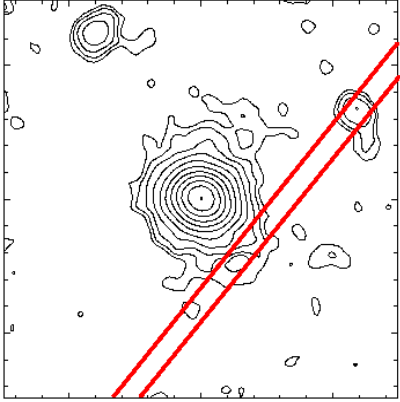


Figure 2. continued.

0204+292 (RQQ) WHT



0230-027 (RG) WHT



0244+194 (RQQ) WHT

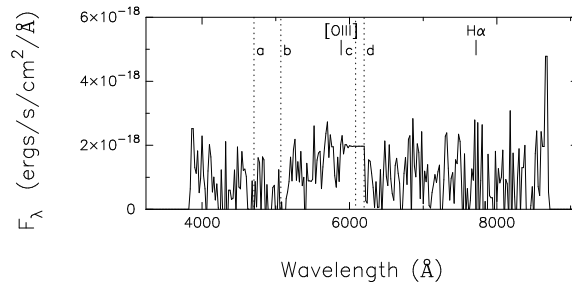
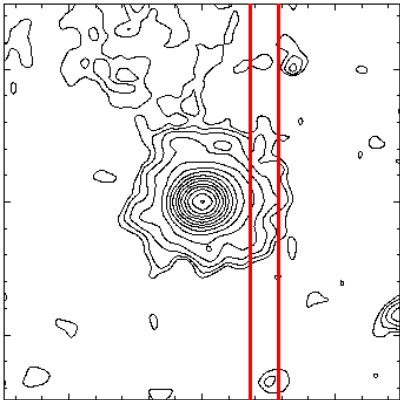
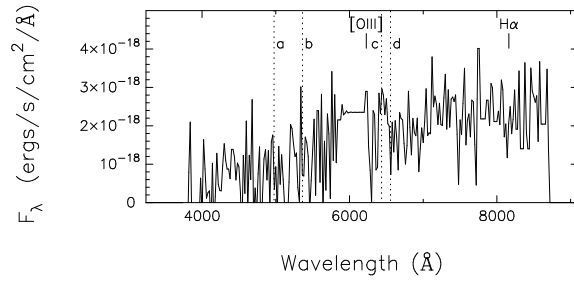
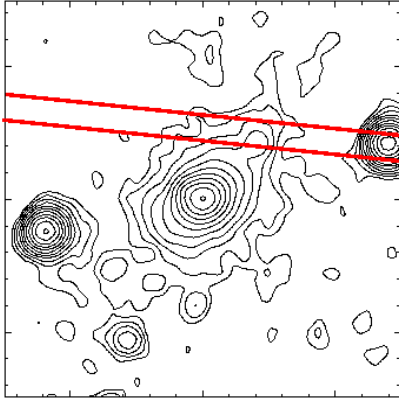
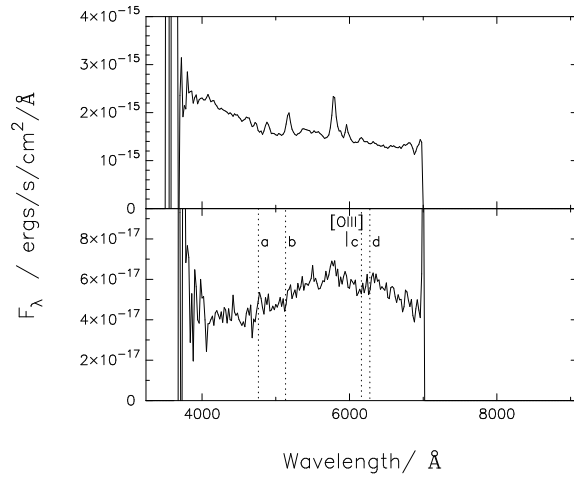
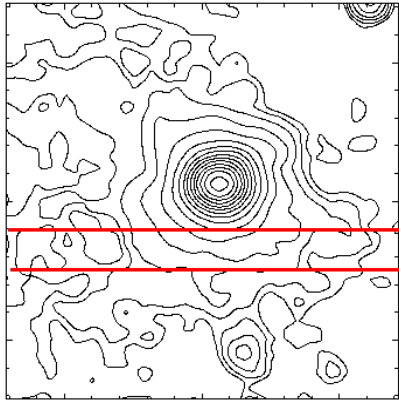


Figure 2. continued.

0345+337 (RG) WHT



0736+017 (RLQ) M4M



0736+017 (RLQ) WHT

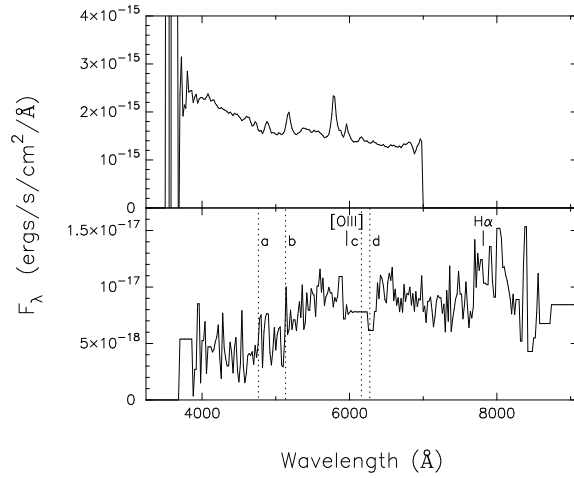
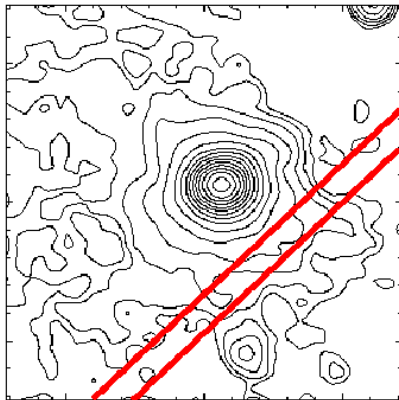
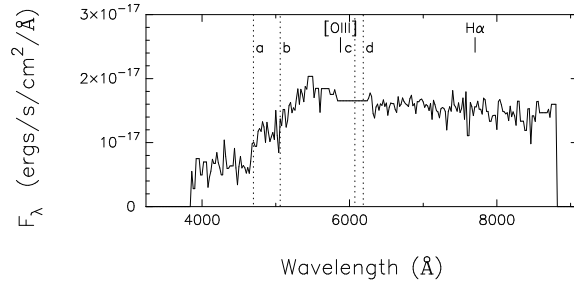
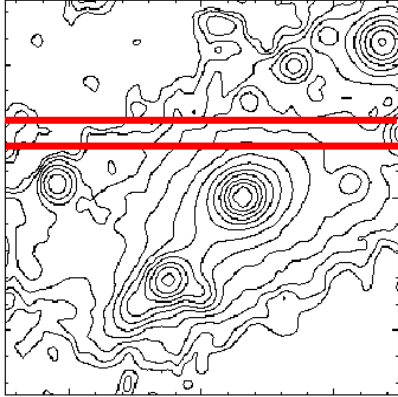
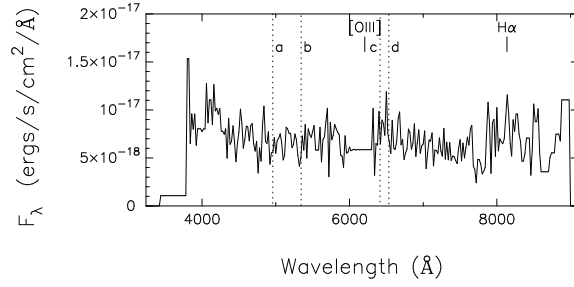
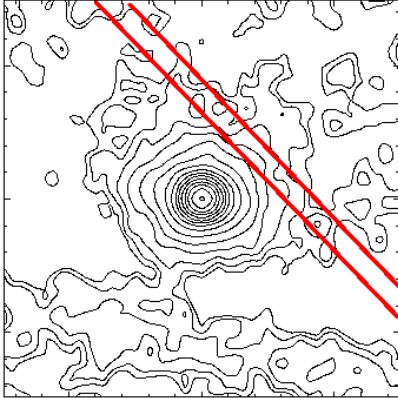


Figure 2. continued.

0917+459 (RG) WHT



1004+130 (RLQ) WHT



1020-103 (RLQ) M4M

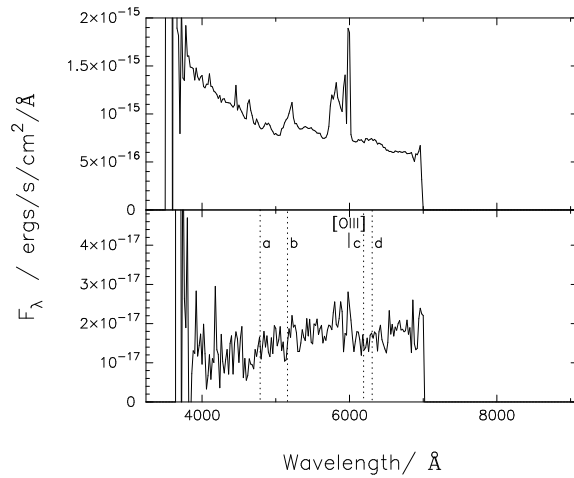
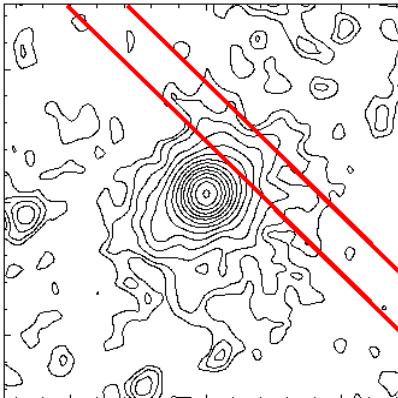
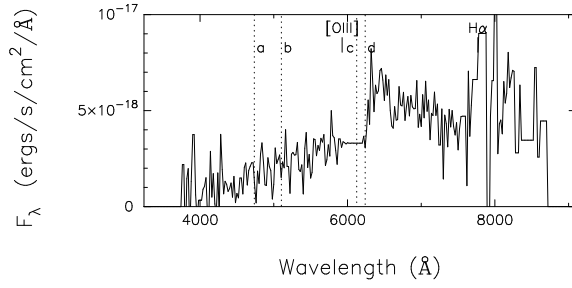
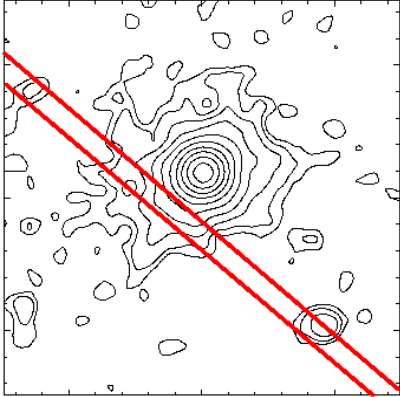
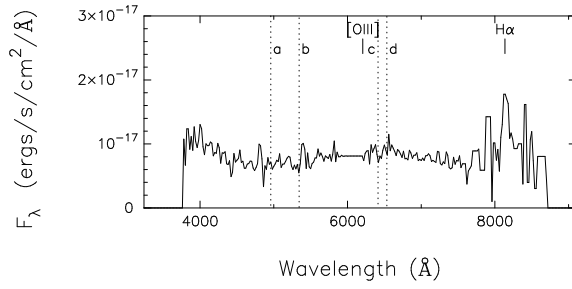
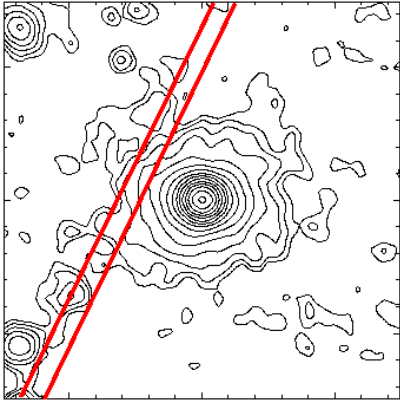


Figure 2. continued.

1215-033 (RG) WHT



1217+023 (RLQ) WHT



1330+022 (RG) M4M

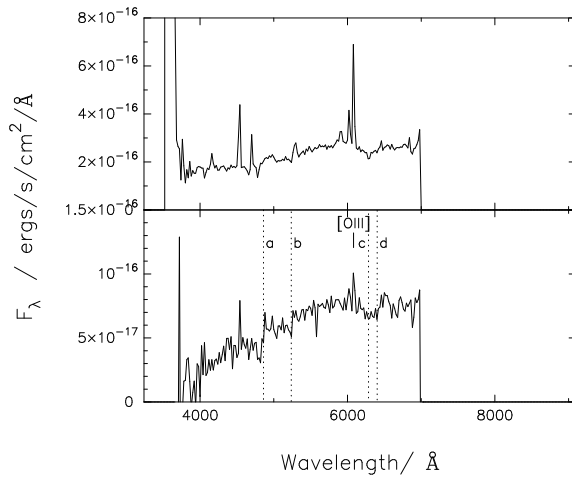
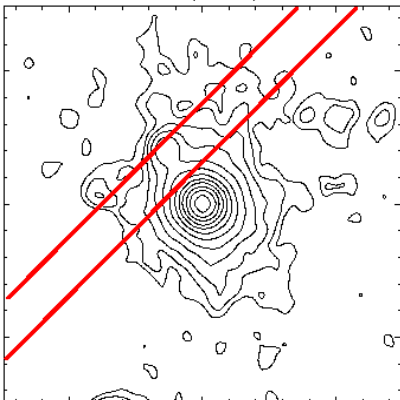
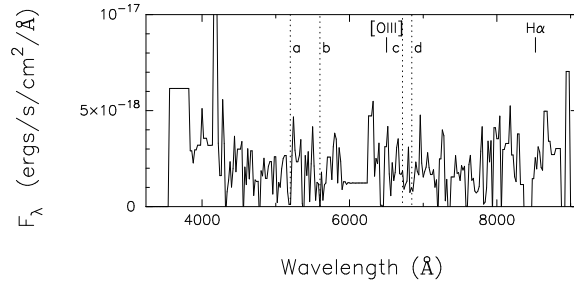
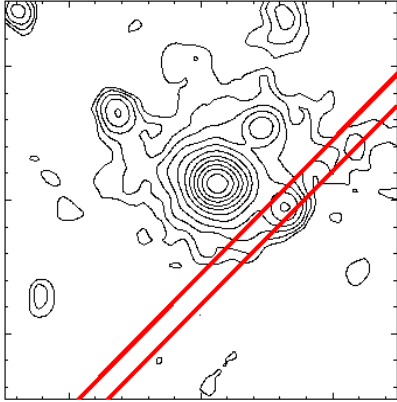
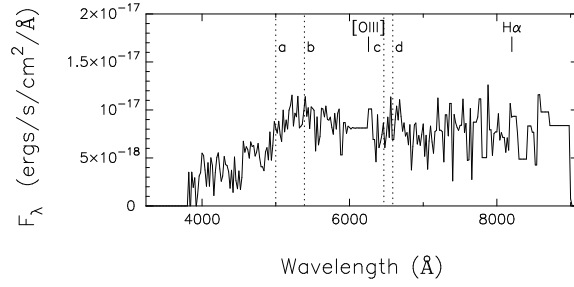
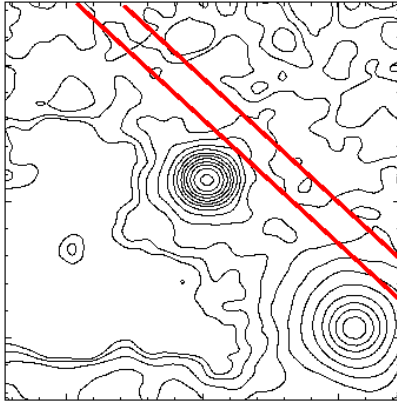


Figure 2. continued.

1334+008 (RG) WHT



1549+203 (RQQ) WHT



1635+119 (RQQ) WHT

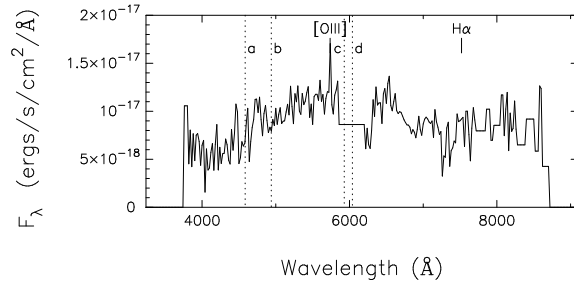
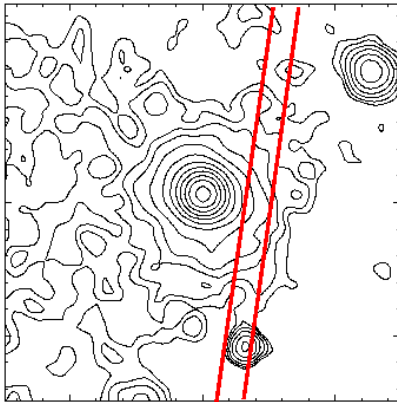
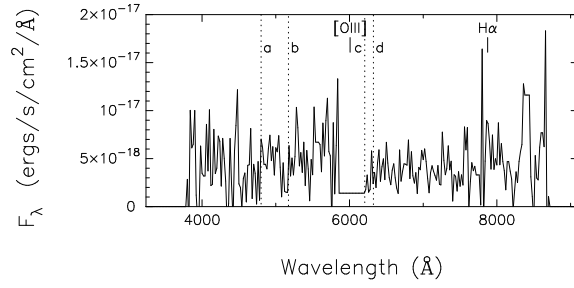
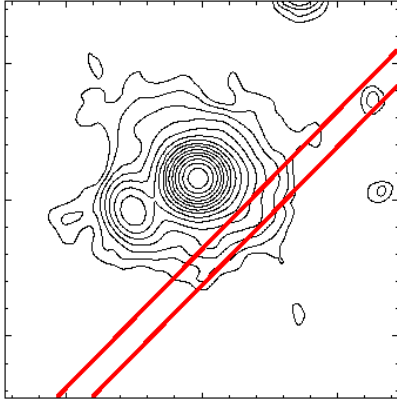
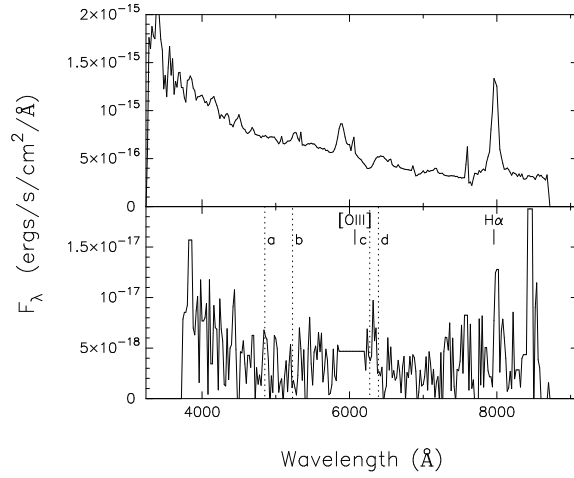
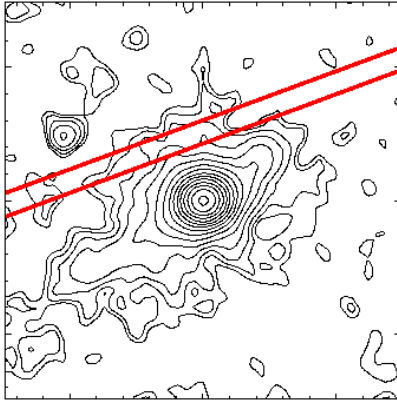


Figure 2. continued.

2135-147 (RLQ) WHT



2141+175 (RLQ) WHT



2141+279 (RG) M4M

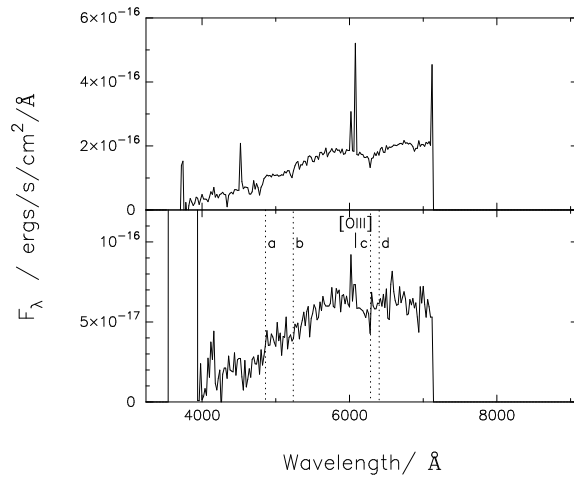
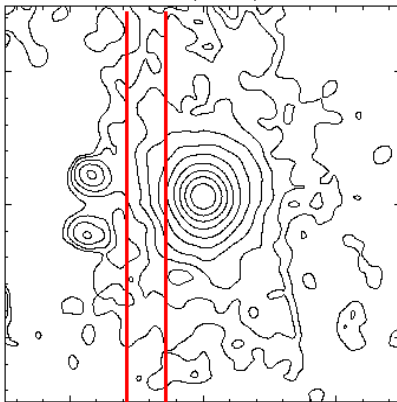
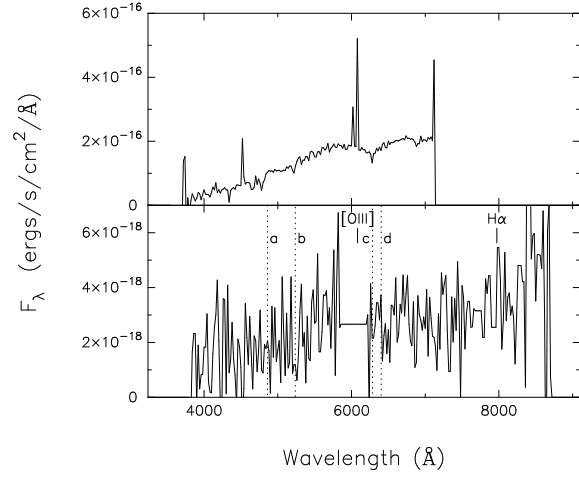
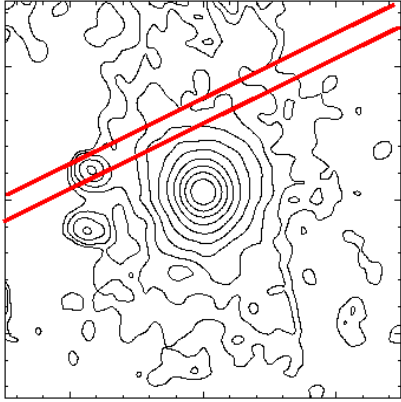
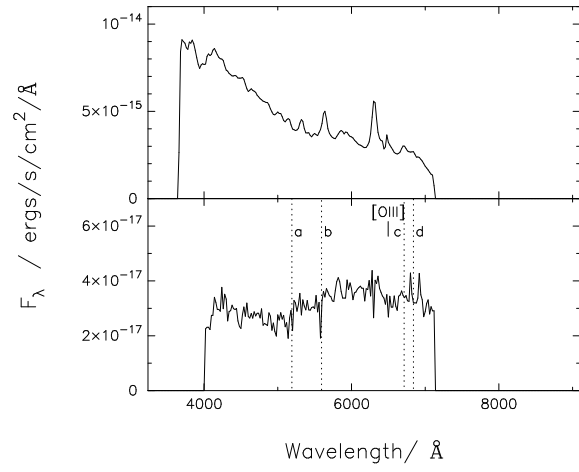
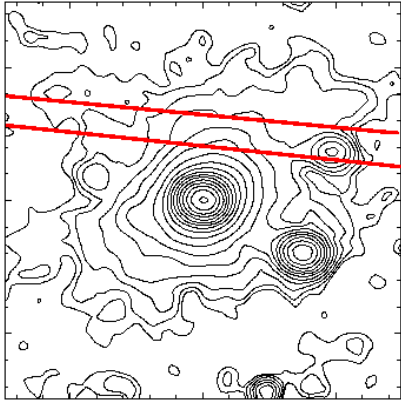


Figure 2. continued.

2141+279 (RG) WHT



2201+315 (RLQ) M4M



2215-037 (RQQ) WHT

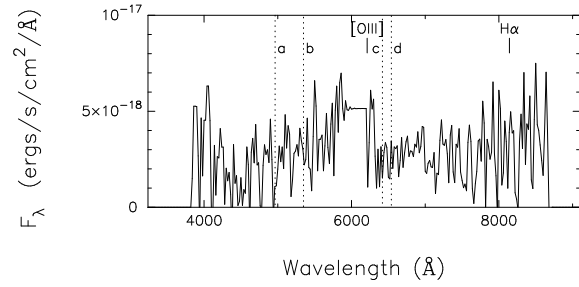
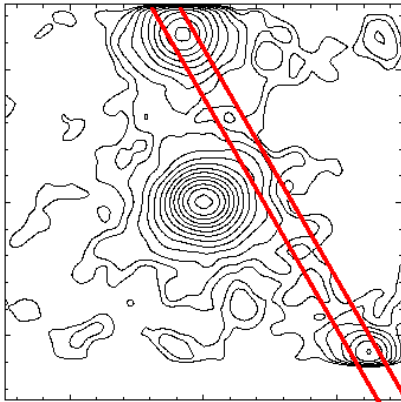
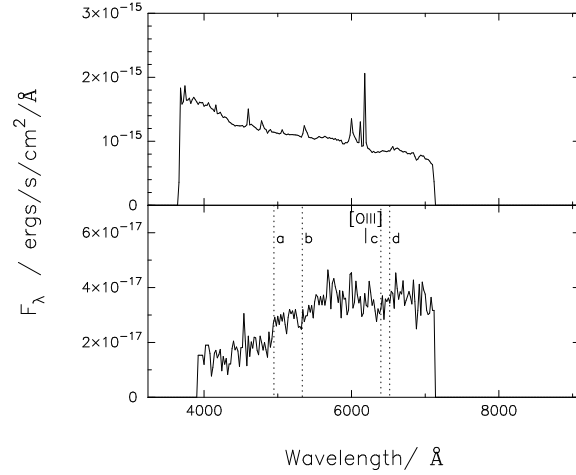
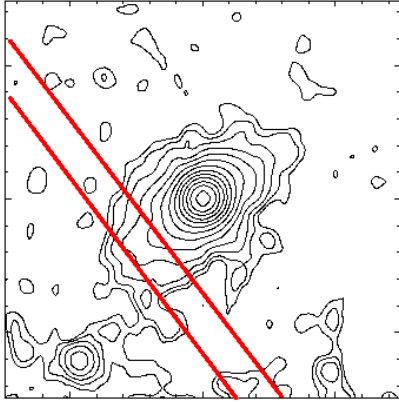
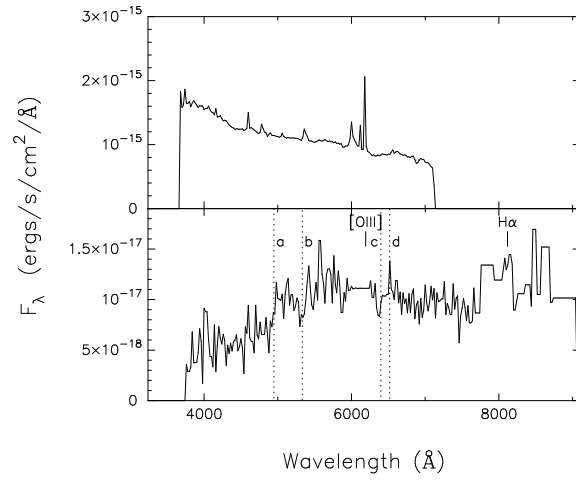
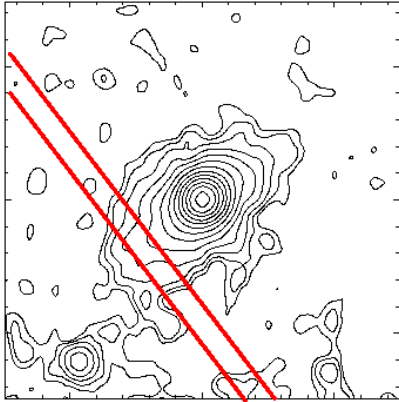


Figure 2. continued.

2247+140 (RLQ) M4M



2247+140 (RLQ) WHT



2344+184 (RQQ) M4M

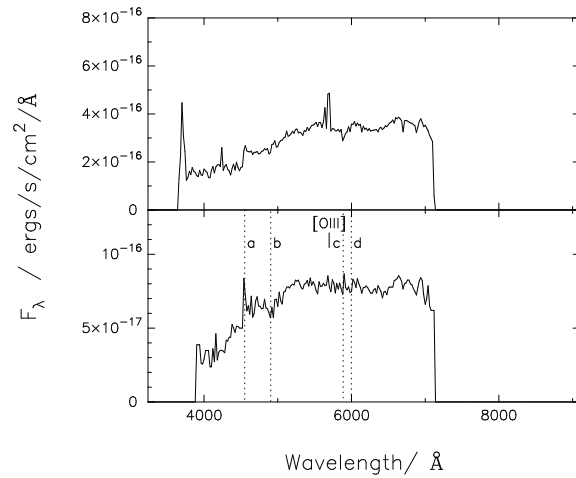
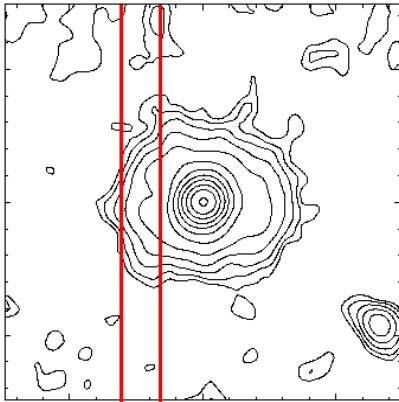
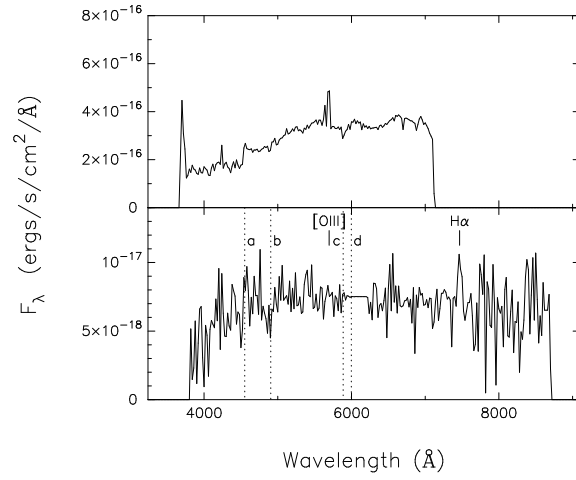
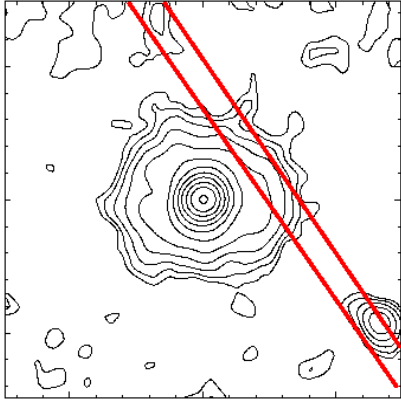


Figure 2. continued.

2344+184 (RQQ) WHT



2349-014 (RLQ) WHT

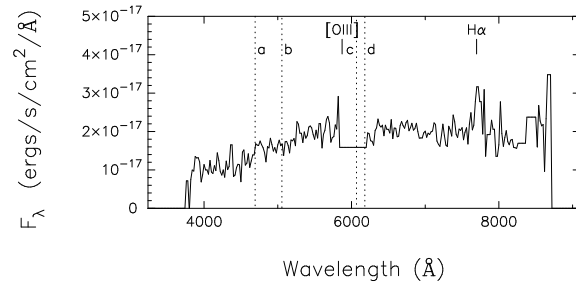
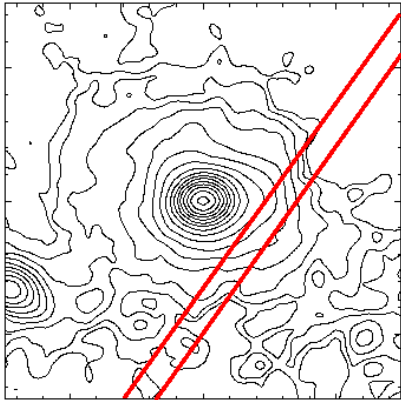


Figure 2. continued.

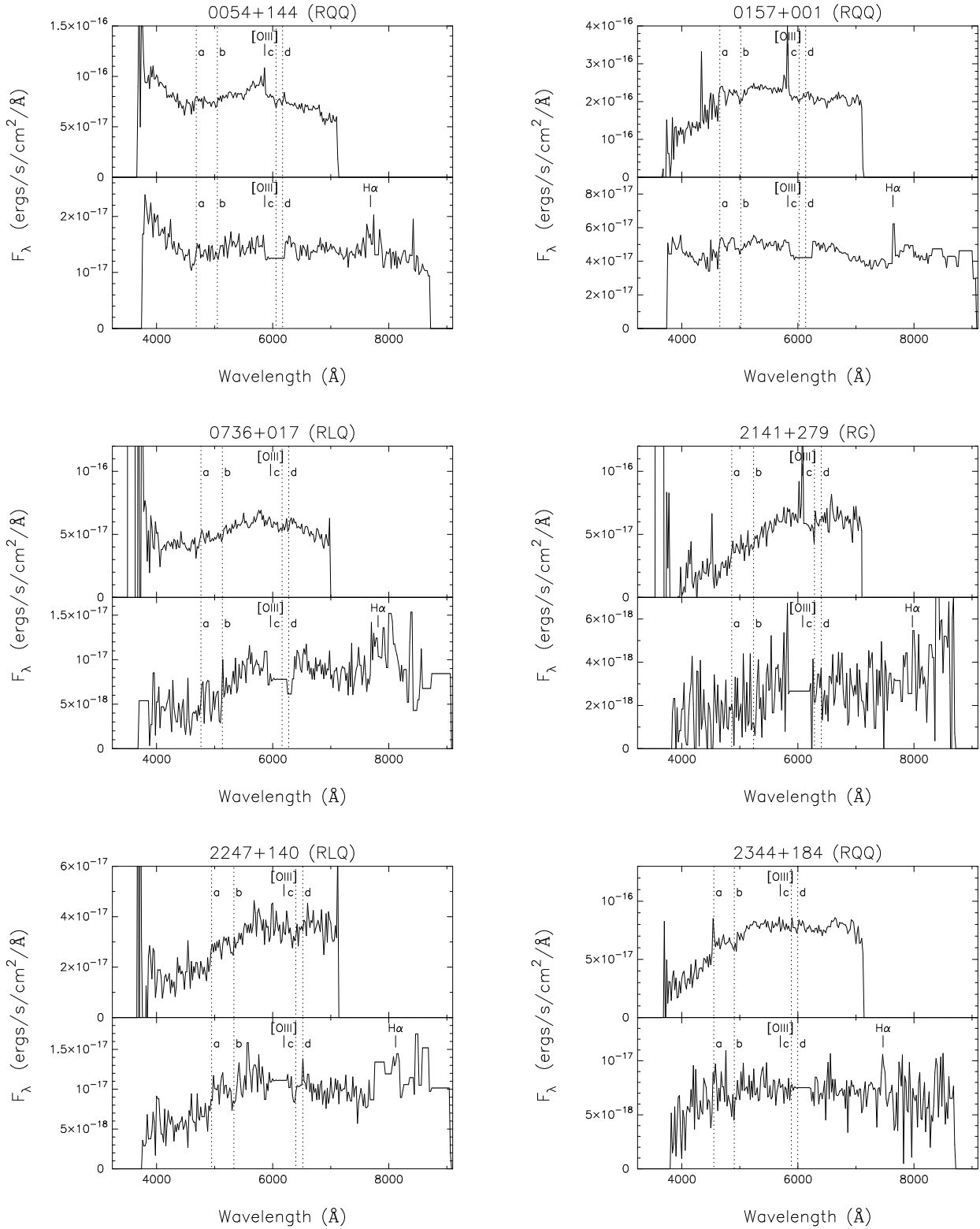


Figure 3. A comparison of off-nuclear (host galaxy) spectra obtained on the Mayall 4-m Telescope at Kitt Peak (upper panel) with those obtained with the 4.2m WHT (lower panel). The spectra are plotted at the observed wavelength in units of F_λ . The expected positions of various stellar absorption features are shown as vertical dotted lines: (a) the 4000 \AA break; (b) G band ($\lambda_{rest} = 4300 \rightarrow 4320\text{\AA}$); (c) Mg Ib ($\lambda_{rest} = 5173\text{\AA}$); (d) Fe λ 5270. The redshifted wavelengths of the [OIII] λ 5007 and H α emission lines are also marked. Different slit widths were used on the two instruments and the flux calibration for the WHT spectra is relative rather than absolute, so the flux values from the two telescopes are not directly comparable.